NACA

RESEARCH MEMORANDUM

AN EMPIRICALLY DERIVED METHOD FOR CALCULATING PRESSURE

DISTRIBUTIONS OVER AIRFOILS AT SUPERCRITICAL MACH

NUMBERS AND MODERATE ANGLES OF ATTACK

By

Gerald E. Nitzberg and Loma E. Sluder

Ames Aeronautical Laboratory
Moffett Field, Calif.

NATIONAL ADVISORY COMMITTEE
FOR AERONAUTICS
WASHINGTON
April 1, 1947

NACA RM. NO. A7B07   CONFIDENTIAL

NATIONAL ADVISORY COMMITTEE FOR AERONAUTICS

RESEARCH MEMORANDUM

AN EMPIRICALLY DERIVED METHOD FOR CALCULATING PRESSURE

DISTRIBUTIONS OVER AIRFOILS AT SUPERCRITICAL MACH

NUMBERS AND MODERATE ANGLES OF ATTACK

By Gerald E. Nitzberg and Loma E. Sluder

SUMMARY

On the basis of an analysis of experimental airfoil data
a procedure is developed for calculating pressure distributions
over airfoils at supercritical Mach numbers. A number of
factors limit application of the method to moderate angles of
attack. Only the forward portion of the airfoil, where
interaction between local boundary-layer thickness and local-
pressure distribution is negligible, is considered in detail.
Use of the method developed merely requires a knowledge of
the low-speed or potential theory, pressure distribution,
and the shape of the airfoil. Calculated and experimentally
measured high-speed pressure distributions are compared for
a wide variety of airfoils at different angles of attack
and Mach numbers.

INTRODUCTION

Air, when flowing past moderately thick airfoil sections
at seven- or eight-tenths the velocity of sound, attains local
velocities in excess of sonic. Analysis of such mixed subsonic
and supersonic types of flow presents difficulties which are
greater than those of either purely subsonic or supersonic
flow.

A general compressibility correction for pressure coef-
ficients has been derived by Kármán and Tsien (reference 1)
which, when applied to potential theory pressure distributions,
gives the distribution over an airfoil in any desired wholly
subsonic flow. In the regime of purely supersonic flow,
Prandtl and Meyer (reference 2) derived a theory of the
pressure distribution over a curved surface by considering
the effects on an initially semi-infinite uniform flow at
sonic velocity when it is deflected around a corner. It
was found that the local supersonic Mach numbers attained by
the stream are a function only of the total angle through
which the stream is turned. This theory can be used to
obtain the pressure distributions over airfoils at supersonic
Mach numbers. The supersonic flow region in the vicinity of
airfoils at high subsonic free-stream Mach numbers is limited
in extent so that the Prandtl-Meyer theory cannot be applied
directly. As a result of mathematical difficulties, a

readily applicable solution of the problem of supersonic
flow of limited extent has not been obtained as yet, but
the importance of the problem makes it expedient to resort
to an empirical analysis.

Pressure distributions over a number of airfoils at high
Mach numbers have recently been obtained in the Ames
1- by 3-1/2-foot high-speed wind tunnel. The airfoils are of
the conventional sections NACA 0015, 23015, 4415 and 4412,
and the low-drag sections NACA 65_2-215 (a = 0.5) and 66,2-215
(a = 0.6). These pressure distributions were obtained at
Reynolds numbers of approximately 2,000,000 and are considered
to be accurate representations of free-air results up to Mach
numbers of 0.810 for moderate angles of attack. The effects
of Reynolds number variation on high-speed pressure distri-
butions are not known. Therefore, it is not possible to
estimate what restrictions are imposed on the generality of
an analysis based on these pressure measurements as a result
of the moderate test Reynolds number.

Experimental section drag coefficients were obtained by
wake surveys simultaneously with the pressure distributions.
At moderate angles of attack, the drag coefficients show no
appreciable variation with Mach number until the local
velocity of sound is exceeded at some point on the airfoil
surface. The free-stream Mach number at which local sonic
velocity first occurs is the critical Mach number. Above

the critical Mach number, there is a more or less marked

increase in the airfoil drag coefficient. Since a drag

increase is indicative of a thickening boundary layer, it is

anticipated that there are considerable boundary-layer

effects at supercritical speeds. It would thus appear

possible to start an analysis of the experimental pressure

distributions by separating the viscosity and compressibility

effects. In reference 3, it is shown that the differences

between airfoil section characteristics in potential flow and

in real viscous fluids can be accurately treated by taking

account of the boundary layer. These differences were found

to be chiefly embodied in effective changes in the airfoil

shape and angle of attack. It thus might be hoped that the

compressible supercritical counterpart of potential theory

could be obtained by correcting the experimental pressure

distributions for the boundary-layer viscosity effects.

Reference 4 has treated the growth and stability of the

laminar boundary layer at large Mach numbers; but a survey

of the literature reveals that boundary-layer changes through

and behind shock waves have not yet been successfully analyzed.

Moreover, there are a number of indications of a strong inter-

action between the shock wave and boundary layer which

eliminates the possibility of separating viscosity and

compressibility effects in the vicinity of the shock wave.

In spite of this limitation, it still seems feasible to

separate gross viscosity effects, such as effective angle-of-attack changes, from the compressibility effects.

The initial step in the procedure used in the present report was the determination of all the known airfoil parameters, that is, the directly determinable properties of the airfoil and the flow field. These parameters were correlated with that property of the pressure distribution under consideration to find the ones which seem relevant. The result of such a procedure is not rigorously correct because it is based only on combinations of those parameters which are available. In other words, if some other parameter could be obtained, a combination of parameters might be found which would give equal or better correlation with the experimental measurements. Thus, the acceptance of the results of this report is dependent upon the rationality of the analysis based upon those parameters which are taken to be of prime importance.

ANALYSIS

At supercritical Mach numbers, where the flow in the vicinity of an airfoil is both subsonic and supersonic, it is to be expected that the relative importance of local airfoil-shape parameters will be different for these two types of flow. Therefore, these two regimes will be considered separately.

Forward Subsonic Region

A procedure for handling the forward subsonic region of the pressure distribution is suggested by analogy with the low-speed theory of viscosity effects on airfoil characteristics. This theory shows that the presence of a thick boundary layer results in an effective change in the angle of attack and camber line. The relatively large drag coefficients at supercritical Mach numbers are indicative of thick boundary layers. Therefore, it is to be expected that there is an effective angle-of-attack change at supercritical Mach numbers.

A study of experimental data at supercritical Mach numbers reveals that, for the airfoils tested, which were of 12- and 15-percent thickness, the subsonic region is of very limited chordwise extent on at least one surface at most angles of attack. In fact, at large Mach numbers the subsonic portion of the pressure distribution over both airfoil surfaces is greater than a few percent of a chord length at only moderate angles of attack, that is, angles from $0°$ to $4°$. So in order to handle the subsonic regime, the analysis will have to be limited to such moderate angles of attack. The primary importance of studying the subsonic portion of the pressure distribution is as a means for predicting the chord-wise location of the point at which sonic velocity is attained. In order to obtain a precedure which can be applied to an

arbitrary airfoil section, it is necessary to relate super-
critical pressure distributions to low-speed pressure
distributions. To do this, it would seem possible to
apply the Kármán-Tsien theory to low-speed pressure
distributions at angles of attack corrected for the high-
speed boundary-layer effects. However, the experimental
observations which are to be discussed directly indicate
that in the immediate vicinity of the airfoil stagnation
point the variation of pressure coefficient with Mach number
does not seem to follow the Kármán-Tsien theory. An
examination of subcritical pressure distributions, at angles
of attack for which the drag coefficient remained constant
with the increasing Mach number, revealed that at $2\frac{1}{2}$- and
5-percent-chord stations the experimental pressure-coeffi-
cient variation with Mach number was less than that
predicted by the Kármán-Tsien theory, while the variation
aft of the 10-percent-chord station was in good agreement
with the theory. At supercritical Mach numbers there are
other factors besides compressibility which affect the
variation with Mach number of pressure coefficients in the
forward subsonic portion of the airfoil so that it was not
feasible to investigate the observed deviation from theory
in detail. Lacking a more appropriate compressibility
correction, the present analysis will apply the Kármán-Tsien
theory even near the airfoil leading edge.

In low-speed viscous theory, an effective angle-of-attack change is considered to occur when the presence of a boundary layer alters the flow past an airfoil in a manner which is similar to that which would arise from a shift of the airfoil trailing edge from its actual physical position to an effective position at the center of the total trailing-edge boundary layer. Thus, to find the effective angle-of-attack change, it is only necessary to know the trailing-edge boundary-layer thickness for each surface of the airfoil. At low speeds the drag coefficient is a known function of boundary-layer thickness and pressure coefficient at the trailing edge. However, this functional relation is not known for super-critical speeds. Moreover, at supercritical Mach numbers, drag has two components - losses through the shock wave and within the boundary layer. It is not to be expected that the shock-wave wake would operate like the boundary layer, in changing the effective angle of attack. Therefore, the trailing-edge boundary-layer thickness cannot be directly determined at supercritical Mach numbers from the known pressure distribution and drag coefficient.

That portion of the experimental pressure distributions ahead of the sonic point was reduced to low speeds by using the Kármán-Tsien theory. When these adjusted pressure distributions were compared with low-speed pressure distri-butions, it was found that the upper and lower surfaces of an

airfoil appeared to be at different angles of attack. The
adjusted pressure distributions over single surfaces did
not conform exactly to the low-speed distribution for any
angle of attack; however, over the forward subsonic portion
of each pressure distribution, the maximum scatter
corresponded to a spread of a few tenths of a degree. This
similarity indicates that, as a first approximation, the
total boundary-layer effect can be treated as an angle-of-
attack change. A precise evaluation of boundary-layer
effects would require separating the angle-of-attack
effect and the shape change. There is no available method
for calculating boundary-layer changes in the vicinity of a
shock wave so the present analysis is limited to the
previously mentioned first approximation.

The effective angle of attack for each airfoil surface
was calculated from the experimental pressure distributions
for which only one surface had a region of supersonic flow.
For the moderate angles of attack considered, the supersonic
region always occurred on the upper surface of the airfoil.
The values of the effective angle-of-attack change, occasioned
by the presence of a shock on the upper surface $\Delta\alpha$ (U.S,S.)
were plotted for each surface as a function of the increment
of the free-stream Mach number above the critical Mach
number $M-M_{cr}$. Values were plotted for the upper surface in
figure 1 and those for the lower surface in figure 2. In these

figures it is seen that for the wide variety of airfoil shapes and differences in free-stream Mach number and geometric angles of attack, the maximum dispersion of the points for any value of $M - M_{cr}$ is only about 1°. Therefore, a curve faired through the mean values of the experimental points can be used to predict the effective angle-of-attack change for a given value of $M - M_{cr}$ to within about 1/2°. Although this approximation is adequate for predicting the sonic-point location, an attempt was made to determine whether this dispersion was a function of some other parameter. A parameter which seemed to be of considerable importance was $dM_{cr}/d\alpha$. It was noticed that the majority of the cases for which $\Delta\alpha(U.S.S.)$ values were low corresponded to configurations having values of $dM_{cr}/d\alpha$ greater than 0.025. Further evidence of the importance of this parameter is presented in figure 3 where the increment of drag coefficient above the low-speed drag coefficient $C_D - C_{D_{L.S.}}$ is plotted as a function of $M - M_{cr}$, for the configurations considered in figures 1 and 2. Figure 3 shows that, for all but one configuration, a curve can be drawn separating the points having large and small values of $dM_{cr}/d\alpha$. A method, based on this parameter, has been developed for predicting the effective angle of attack with greater accuracy; however, the theoretical critical Mach numbers are not in sufficiently close agreement with experimentally measured values to justify the use of this

more involved method.

The critical Mach number of an airfoil at a given geo-
metric angle of attack can be found by applying the Kármán-
Tsien compressibility correction to the airfoil peak-pressure
coefficient obtained from potential theory. This procedure
has been used in reference 5. It is found that the variation
of critical Mach number of each surface of an airfoil with
angle of attack is different for airfoils of different shapes,
and, even for a given airfoil, there are two markedly different
angle-of-attack regimes for each surface in which this differ-
ence in variation is apparent. One regime, usually positive
angles of attack for lower surfaces and negative angles for
upper surfaces, includes angles for which the peak-pressure
coefficient is determined chiefly by the airfoil-thickness
distribution and camber, and consequently there is little
change of critical Mach number with angle of attack. In the
other regime, the maximum-pressure peak occurs near the air-
foil nose as a result of the additional lift distribution,
that is, the increased circulation resulting from pitching
the airfoil. There is considerable uncertainty as to the
accuracy of the calculations of critical Mach numbers at
these angles because of the previously discussed deviation
of the flow near the stagnation point from the Kármán-Tsien
theory. In this regime, uncertainty also exists for critical
Mach numbers determined from high-speed experimental pressure
distributions unless a number of pressure orifices have been

pl∼.ccd along the forward 5 percent of the airfoil chord. This limitations places serious restriction on a significant source of information regarding the high-speed characteristics of airfoils.

The experimental and theoretical critical Mach number curves for both surfaces of the airfoils considered are shown as a function of angle of attack in figure 4. As will be discussed directly, in the present method of analysis, a correction to the theoretical curves is required.

When only one surface is at a supercritical Mach number there is an effective angle-of-attack change of the other surface which results in a change in the pressure distribution and thus in the critical Mach number of the latter surface. Therefore, if the critical Mach number curves are obtained theoretically, it is necessary to adjust the calculated values for the surface with the higher critical Mach number to account for the effective angle-of-attack change due to the shock wave on the other surface of the airfoil. Curves thus derived are in reasonable agreement with experimental measurements.

As was indicated previously, when the free-stream Mach number M is above the critical Mach number of only one surface of an airfoil, the following procedure can be used to calculate the subsonic portion of the pressure distribution over the airfoil. The critical Mach number M_{cr}, for the moderate geometrical angle of attack under consideration, is computed from the low-speed pressure

distribution by means of the Kármán-Tsien theory. Curves of
the Kármán-Tsien compressibility correction are given in
figure 5. Then having the value of $M - M_{cr}$, the curve of
figure 1 is used to estimate the effective angle of attack
for the surface of the airfoil over which the local region
of supersonic flow occurs. The subsonic portion of the
pressure distribution over this surface of the airfoil at
the free-stream Mach number under consideration is obtained
by applying the Kármán-Tsien compressibility correction to
the low-speed pressure distribution corresponding to the
effective angle of attack. The flow over the other airfoil
surface is entirely subsonic so that the pressure distri-
bution can be estimated directly. The effective angle of
attack of this surface is obtained from the curve of figure 2
by using the same value of $M - M_{cr}$ as used in figure 1.

The previously mentioned procedure can be generalized to
apply to the case of airfoils at Mach numbers above the
critical speed of both surfaces if the assumption is made
that the effects of the supersonic region on each surface
are additive. In this case, it is necessary to obtain the
critical Mach number for each surface of the airfoil. Then
using the upper-surface Mach number increment above its
critical $(M - M_{cr_U})$ the effective angle-of-attack changes,
due to the upper-surface supersonic region of flow, for the
upper surface $\Delta\alpha(U.S.S.)_U$ and lower surface $\Delta\alpha(U.S.S.)_L$

of the airfoil are obtained from figures 1 and 2, respectively.
Similarly, for the lower-surface increment above its critical
$(M - M_{cr_L})$ the effective angle-of-attack changes, due to the
lower-surface supersonic region of flow, for the lower surface
$\Delta\alpha(L.S.S.)_L$ and upper surface $\Delta\alpha(L.S.S.)_U$ are obtained from
figures 1 and 2, respectively. The total effective angle-of-
attack change is then $\Delta\alpha(U.S.S.)_U - \Delta\alpha(L.S.S.)_U$ for the upper
surface, and $\Delta\alpha(U.S.S.)_L - \Delta\alpha(L.S.S.)_L$ for the lower surface.

The limited experimental data used to derive the afore-
mentioned general procedure make it of dubious accuracy at
Mach numbers above $M - M_{cr}$ of 0.20. Below this limit the
maximum difference between the calculated angle of attack of
a surface, predicted by this procedure, and that obtained from
the experimental pressure distribution was about 1/2°.

The preceding method can be used to predict the chordwise
location of the point at which sonic velocity is first attained.
The pressure coefficient corresponding to sonic velocity at a
given free-stream Mach number may be obtained from figure 5.
The movement of the sonic point with Mach number has been
predicted using this procedure for the airfoils for which
experimental pressure distributions are available. The method
is applicable for the normal operating range of high-speed
airplanes, that is, angles of attack from 0° to 4° and Mach
number increments less than 0.20 above the critical. In
this range the difference between the calculated value and

the experimentally measured sonic point was less than a few
percent of a chord length.

Region of Increasing Supersonic Local Mach Numbers

The Kármán-Tsien compressibility correction is strictly
limited to subsonic regions of the pressure distribution.
The only available procedure for supersonic flows is that of
Prandtl and Meyer, which presents the local Mach number as a
function of the difference between the local surface slope
and the slope at the sonic point. The local Mach number is
uniquely related to the pressure coefficient for a given
free-stream Mach number. This relationship is shown in
figure 6. To study the supersonic portion of the airfoil
pressure distribution at moderate angles of attack, local
Mach number was plotted as a function of the change in slope
of the surface from that at the sonic point. It was found
that the variation was similar to the Prandtl-Meyer theory
but different configurations achieved varying percentages
of the theoretical local Mach number rise above unity
corresponding to a given slope change. The Prandtl-Meyer
theoretical increase in local Mach number for expansive
deflection of the stream from its direction at sonic
velocity and several percentages of this theoretical
variation are presented in figure 7. For a given airfoil,
angle of attack, and Mach number, the local Mach numbers

attained conformed closely to a unique percentage of the
Prandtl-Meyer theoretical results. This failure to obtain the
full theoretical rise of local Mach number seems reasonable
because the Prandtl-Meyer theory is based on the assumption
of a semi-infinite uniform sonic flow deflected around a
curved surface; whereas, airfoils at supercritical Mach
numbers have a supersonic region of very limited extent. The
extent and uniformity of this supersonic region depends on
such factors as the free-stream Mach number, the critical
Mach number, and the chordwise location of the sonic point.

One variable chosen was "Percent of Prandtl-Moyer" and
this was correlated with all known airfoil parameters which
seemed relevant. These parameters included $M - M_{cr}$, the
surface curvature at the sonic point and also at the point at
which a local Mach number of 1.2 occurs, the slope of the
airfoil surface at the sonic point relative to the free-
stream direction and also relative to the airfoil chord line,
the chordwise location of sonic velocity and local Mach number
of 1.2, and others. It was found that the two parameters
which gave the best correlation with percent of Prandtl-Meyer
were $M - M_{cr}$ and the slope of the surface at the sonic point
relative to the airfoil chord line. Measuring slope relative
to the airfoil chord line seems strange at first consideration
but, since for the configurations considered, the stagnation
point very nearly coincides with the forward end of the chord

line, there seems to be some physical basis for using the airfoil chord as a reference line. The data which were analyzed included cases for which the included angle θ_S between a tangent to the surface at the sonic point and the airfoil chord line varied from 5° to 30°. Within this range it was observed that for equal values of $M - M_{cr}$ the percent of Prandtl-Meyer attained decreased with increasing θ_S. It should be mentioned that increasing values of θ_S correspond to movement of the sonic point toward the airfoil leading edge. The other variation noted was that increasing $M - M_{cr}$ for constant values of θ_S resulted in increasing the percent of Prandtl-Meyer which was attained. Curves based on the experimental data are presented in figure 8. The maximum difference between experimental values and these curves corresponded to a 5-percent shift in percent of Prandtl-Meyer.

Once the slope distribution over the airfoil and the sonic-point location are determined, the supersonic portion of the pressure distribution can be calculated as follows: The percentage of the Prandtl-Meyer theoretical curve which should be used is determined from figure 8. The local Mach numbers reached at any chordwise station are obtained from the particular percentage curves shown in figure 7. When the curves of figure 6 are used, these local Mach numbers can be converted directly to pressure coefficients S.

Of course, this analysis is based on the use of percent of Prandtl-Meyer as a parameter and thus can only be considered to be empirically derived.

Termination of the Supersonic Regime

There is nothing in the foregoing analysis to give any clue as to the chordwise point of termination of the supersonic region. It was believed that there was a very direct relation between the stability of the boundary layer and the location of the shock wave. To check this hypothesis, pressure distributions over a carefully cleaned NACA 4412 airfoil were obtained at a moderate angle and various Mach numbers in the Ames 1- by 3-1/2-foot high-speed wind tunnel. Then grains of carborundum were attached between the 5- and 10-percent chordwise stations on the airfoil, and pressure distributions at the same angle and Mach numbers were obtained. The pressure recovery, corresponding to the shock wave, was much more abrupt but only slightly further forward for the roughened airfoil than for the smooth airfoil. The pressure distribution in the region of increasing supersonic local Mach numbers was the same for the two airfoil surface conditions. It is not feasible to make a quantitative analysis of this phenomenon since there are no available theories of laminar separation, transition from laminar to turbulent boundary-layer flow, or turbulent separation, in supersonic flows.

Even more important, there are no quantitative results for
the interaction between such boundary-layer changes and shock
waves. For the pressure distributions available on airfoils
of 12- and 15-percent thickness, for moderate angles of
attack at Mach numbers between 0.05 and 0.20 above the
critical, it was noticed that the point at which the local
supersonic Mach numbers ceased to increase corresponded
roughly to that point, on the surface under consideration,
at which the surface was tangent to the free-stream direction.
It is not immediately apparent why this geometrically deter-
mined parameter should so influence the flow past the airfoil.

There is usually no precise location of a shock wave
discernible from the pressure distributions. Instead of an
abrupt discontinuity there is a gradual pressure recovery.
These pressure distributions were obtained by means of a
liquid manometer so that they may represent a time average
pressure distribution of an unsteady flow condition.
Alternatively, the gradual pressure recovery observed may be
a result of a thick boundary layer. This boundary layer may
soften the shock as discussed in reference 6. Also, the
abrupt pressure change might be masked by the boundary-
layer thickness, but this seems unlikely since, as has
been previously mentioned, an abrupt pressure recovery was
observed on the roughened NACA 4412 airfoil. It is expected
that, since airfoil surface roughness causes marked changes

in the nature of the pressure recovery which accompanies
transition from supersonic to subsonic flow, Reynolds number
might have important effects on the shock wave. In all the
configurations analyzed it was found that the position on the
airfoil surface at which the local Mach number had dropped to
unity could be estimated by applying the Kármán-Tsien
compressibility correction to the potential theory pressure
distribution. It was therefore decided to terminate the
supersonic portion of the pressure-distribution calculations
at the chordwise station for which a local Mach number of
unity is predicted.

The experimental pressure distributions indicate a more or
less gradual pressure recovery over the region from the chord-
wise station at which the surface is tangent to the free-
stream direction to that station at which a local Mach number
of unity occurs. When the local pressure coefficients for
these two stations are connected by a straight line, it is
noticed that the local portion of the experimental pressure
distribution lies near this line or between this line and the
calculated supersonic pressure distribution. The presence of
this region of decreasing supersonic local Mach numbers is
believed to be due to interaction between the local boundary
layer and the shock wave.

Estimation of Pressure Distribution Aft
of Supersonic Region

Over the rear portion of an airfoil, behind a shock wave, the boundary layer is probably quite thick. It is to be expected that a thick boundary layer could have considerable effect on the local pressure distribution. However, there are no available methods for calculating the boundary-layer thickness behind a shock wave. Therefore, in the present report the subsonic portion of the pressure distribution over the rear of the airfoil will be approximated by applying the Kármán-Tsien compressibility correction to the local potential theory pressure distribution.

DISCUSSION

The primary concern of the preceding analysis is the prediction of supercritical pressure distributions over the forward portion of airfoils. The detailed analysis is restricted to this portion of the airfoil where local boundary-layer thickness does not markedly alter the local pressure distribution. Before comparing calculated and experimental pressure distributions, some of the general problems which arise will be reviewed.

In comparing the low-speed or potential theory pressure distribution to those at moderately high Mach numbers, it is found, as would be expected, that the Kármán-Tsien theory

is inaccurate near the nose of the airfoil. There is no
available procedure for treating this region. Therefore, in
the preceding analysis the assumption is made that the Kármán-
Tsien theory provides an adequate approximation for pressure
coefficients at points close to the airfoil leading edge.
However, the errors introduced by the assumption are of secondary
importance at moderate angles of attack. An investigation is
needed to determine how pressure coefficients change with Mach
number at the nose of the airfoil.

The airfoil-surface slope changes rapidly in the vicinity
of the airfoil nose. When the sonic point occurs in this region,
there may be considerable error in the determination of the
surface slope at the sonic point. Fortunately, the present
method compensates for errors in the sonic-point slope. For
example, if too large a sonic-point slope is read for a given
value of $M - M_{cr}$, too small a percentage of Prandtl-Meyer
theory would be obtained from figure 8. Since local Mach number
attained varies with both the surface-slope change from the sonic
point and the percent of Prandtl-Meyer, and an excessive value
of one results in a diminished value of the other, it is seen
that these two effects tend to counterbalance each other, except
in the immediate vicinity of the sonic point.

The present method can be expected to give rather good
accuracy in determining the peak-pressure coefficients and the
maximum load obtained on the forward portion of the airfoil.

However, a factor which may contribute to differences between calculations and experimental measurements for airplane wings is the fact that the supersonic portion of the pressure distribution depends upon the airfoil-surface slope. As a result of practical construction difficulties, there are discrepancies in the actual wing profile which give rise to uncertainties regarding the surface slope.

Application of Method

In order to evaluate the utility and limitations of the procedure which has been developed, this method has been used to calculate the various configurations for which experimental results are available. As has been pointed out, the development of the method limits its application to moderate angles of attack and to Mach numbers less than 0.20 above the critical Mach number. For angles of 0°, 2°, and 4°, two supercritical Mach numbers have been considered for each airfoil. The calculated characteristics of all the configurations are tabulated in table I.

For incompressible potential theory, it is usual to obtain the velocity distribution rather than the pressure distribution. The additional lift due to pitching the airfoil is directly additive to the basic velocity distribution so that the velocity distribution is particularly convenient for treating cases for which several angles of attack are considered. Since velocity distribution is so easily modified, it was decided to use the

pressure coefficient S, which, at low speeds, is the square of
the ratio of the local velocity and the free-stream velocity.
In figure 5 the Kármán-Tsien theoretical variation of pressure
coefficient S with Mach number is presented. The supersonic
theory of Prandtl-Meyer is in terms of the local Mach number.
Figure 6 gives the pressure coefficient S corresponding to a
local Mach number as a function of free-stream Mach number.

As has been previously mentioned, it was noticed that the
termination of the supersonic regime of rising pressure coef-
ficients occurs approximately at the point where the airfoil
surface is parallel to the effective free-stream direction. In
the calculated pressure distributions this point is connected
with the rearward sonic point by a straight line.

As an example of pressure-distribution variation with
Mach number for a fixed geometric angle of attack the NACA
65_2-215 airfoil at 2° is considered. Figure 9 shows a com-
parison of the calculated pressure-distribution curves and
the experimental points at Mach numbers of 0.700, 0.725,
0.750, 0.775, 0.800, and 0.825. The present method has a
lower limit of applicability at $M - M_{cr}$ of 0.05 because of
the very limited supersonic region for such slightly super-
critical Mach numbers. An approximate value of the pressure
distribution in this regime is obtained by applying the
Kármán-Tsien compressibility correction for the entire
pressure distribution. At Mach numbers of 0.775 and 0.800

the lower surface is only slightly supercritical and applying

the Kármán-Tsien theory gives inaccurate values for the peak-

pressure coefficients. Both surfaces are well above their

respective critical Mach numbers at 0.825 so the present

method can be applied to both surfaces. The large drag

coefficient at this Mach number indicates a thick boundary

layer at the rear of the airfoil which may be the cause of

poor accuracy of Kármán-Tsien theory in this region. Through-

out the Mach number range the calculations give a good

prediction of the peak-pressure coefficients and of the load

over the forward 40 percent of the chord length.

Now consider the same airfoil at different angles of

attack. At 0° and 4°, the marked difference in the type of

loading for the low and high supercritical Mach numbers is

correctly represented by the calculations.

In figure 10, it is seen that the method works well for

the NACA 66,2-215 airfoil at 0° and 2°. As a result of the

small leading-edge radius of this airfoil the upper-surface

critical speed at 4° is determined by a pressure peak near

the nose; therefore, the critical speed cannot be determined

accurately. However, this is a borderline case in that the

forward pressure peak is not very sharp, so the critical Mach

number was based on the farthest forward experimental pressure

point. The calculated pressure distributions based on this

critical Mach number are presented to show the magnitude of

the error that can be expected for such borderline cases.

For the NACA 4412 airfoil at 0°, 2°, and 4° the change in type of loading with Mach number is accurately predicted.

There was some inaccuracy in the construction of the NACA 0015 airfoil as can be seen in figure 12 from the difference between the experimental pressure distribution for the two surfaces at 0°. At 2° for M = 0.725 and at 4° for both Mach numbers shown, the upper-surface shock is very far forward. The start of the marked pressure recovery is still at the point at which the airfoil surface is tangent to the free-stream direction.

The comparisons of experiment and theory for the NACA 23015 are presented in figure 13. At 0°, 2°, and 4° the shock occurs far forward, but the load distribution and pressure peaks are well represented.

It is interesting to notice the similarity between the results for the NACA 4415 airfoil in figure 14 and the NACA 4412 in figure 11. The values of $M - M_{cr}$ used in figure 14 were chosen to be as close as possible to those for the corresponding angles of attack in figure 11. The agreement between calculation and experiment in the vicinity of the nose is not as good for the NACA 4415 airfoil as for the NACA 4412 airfoil because of the difficulty arising as a result of the large leading-edge radius of the former airfoil.

CONCLUDING REMARKS

The procedure which has been developed provides a satis-
factory prediction of the supersonic portion of the super-
critical pressure distributions for airfoils at moderate
angles of attack. The parameters on which the procedure
is based were limited to those which were determinable
from potential theory pressure distributions and the
geometric properties of the airfoils. This method, therefore,
cannot be considered definitive. It is primarily a useful
means for predicting maximum loads and peak-pressure coeffi-
cients. Further experimental investigation of conditions in
the vicinity of the airfoil nose at high Mach numbers should
permit an extension of the method to a wider angle-of-attack
range.

Ames Aeronautical Laboratory,
    National Advisory Committee for Aeronautics,
        Moffett Field, Calif.

Gerald E. Nitzberg,
Aeronautical Engineer.

Loma E. Sluder,
    Physicist.

Approved:

Donald H. Wood,
Aeronautical Engineer.

REFERENCES

1. von Kármán, Th.: Compressibility Effects in Aerodynamics.
   Jour. Aero. Sci., vol. 8, no. 9, July 1941, pp.337-356.

2. Taylor, G. I., and Maccoll, J. W.: Two-Dimensional Flow
   at Supersonic Speeds. Vol. III, div. H, ch. IV of
   Aerodynamic Theory, W. F. Durand, ed., Julius Springer
   (Berlin), 1935.

3. Nitzberg, Gerald E.: The Theoretical Calculation of Air-
   foil Section Coefficients at Large Reynolds Numbers.
   NACA ACR No. 4I12, 1944.

4. Allen, H. Julian, and Nitzberg, Gerald E.: The Effect of
   Compressibility on the Growth of the Laminar Boundary
   Layer on Low-Drag Wings and Bodies. NACA ACR, Jan. 1943.

5. Heaslet, Max. A.: Critical Mach Numbers of Various Air-
   foil Sections. NACA ACR No. 4G18, 1944.

6. Donaldson, Coleman duP.: Effects of Interaction Between
   Normal Shock and Boundary Layer. NACA CB No. 4A27,
   1944.

TABLE I.- SUPERCRITICAL-PRESSURE-DISTRIBUTION PARAMETERS

Airfoil section	α (deg)	M	Exp. M_{cr} Upper surface	Lower surface	M - M_{cr} Upper surface	Lower surface	Δσ (U.S.S.) Upper surface	Lower surface	Δα(L.S.S.) Upper surface	Lower surface	Δα_total Upper surface	Lower surface	θ_sonic Upper surface	Lower surface	Percent Upper surface	P - M Lower surface
65₂-215	2	0.700	0.650	0.760	0.050	----	0.7	0.1	----	----	0.7	0.1	11.9	----	35	---
		.725	.650	.760	.075	----	1.2	.3	----	----	1.2	.3	15.0	----	37	---
		.750	.650	.760	.100	----	1.7	.6	----	----	1.7	.6	15.5	----	40	---
		.775	.650	.760	.125	0.015	2.3	.9	0	.2	2.3	.7	14.5	----	44	---
		.800	.650	.760	.150	.040	2.9	1.3	.1	.6	2.8	.7	13.0	----	48	---
		.825	.650	.760	.175	.065	3.5	1.9	.2	1.0	3.3	.9	13.5	5.5	51	42
	0	.750	.670	.750	.080	----	1.3	.3	----	----	1.3	.3	8.5	----	43	---
		.800	.670	.750	.130	.050	2.4	1.0	.1	.7	2.3	.3	9.0	13.1	51	35
	4	.725	.620	.775	.105	----	1.8	.6	----	----	1.8	.6	22.5	----	36	---
		.800	.620	.775	.180	.025	3.6	2.0	.1	.3	3.5	1.7	18.5	----	46	---
66,2-215	0	.750	.690	.760	.060	----	.9	.2	----	----	.9	.2	7.0	----	40	---
		.800	.690	.760	.110	.040	1.9	.7	.1	.6	1.8	.1	8.6	----	48	---
	2	.750	.670	.770	.080	----	1.3	.3	----	----	1.3	.3	15.5	----	38	---
		.800	.670	.770	.130	.030	2.4	1.0	.1	.4	2.3	.6	15.4	----	43	---
	4	.725	.620	.770	.105	----	1.8	.6	----	----	1.8	.6	28.0	----	34	---
		.800	.620	.770	.180	.030	3.6	2.0	.1	.4	3.5	1.6	20.0	----	45	---
4412	0	.760	.635	.725	.125	.035	2.3	.9	.1	.5	2.2	.4	16.0	----	43	---
		.810	.635	.725	.175	.080	3.5	1.9	.3	1.3	3.2	.6	15.0	36.0	49	31
	2	.700	.595	.775	.105	----	1.8	.6	----	----	1.8	.6	22.0	----	37	---
		.790	.595	.775	.195	.015	4.0	2.5	0	.2	4.0	2.3	18.0	----	48	---
	4	.650	.560	.810	.090	----	1.5	.4	----	----	1.5	.4	34.0	----	32	---
		.750	.560	.810	.190	----	3.9	2.3	----	----	3.9	2.3	25.0	----	43	---
0015	0	.775	.700	.700	.075	.075	1.2	.3	.3	1.2	.9	-.9	15.0	15.0	37	37
		.800	.700	.700	.100	.100	1.7	.6	.6	1.7	1.1	-1.1	18.4	18.4	38	38
	2	.725	.650	.750	.075	----	1.2	.3	----	----	1.2	.3	22.0	----	34	---
		.800	.650	.750	.150	.050	2.9	1.3	.1	.7	2.8	.6	18.4	14.5	43	34
	4	.675	.570	.770	.150	----	1.8	.6	----	----	1.8	.6	39.0	====	31	---
		.750	.570	.770	.180	----	3.6	2.0	----	----	3.6	2.0	35.0	----	35	---
23015	0	.725	.635	.740	.090	----	1.5	.4	----	----	1.5	.4	21.5	----	35	---
		.800	.635	.740	.165	.060	3.2	1.6	.2	.9	3.0	.7	23.0	8.8	42	39
	2	.675	.580	.765	.095	----	1.6	.5	----	----	1.6	.5	28.5	----	33	---
		.750	.580	.765	.170	----	3.4	1.8	----	----	3.4	1.8	28.5	----	39	---
	4	.650	.535	.775	.115	----	2.0	.8	----	----	2.0	.8	32.0	----	33	---
		.725	.535	.775	.190	----	3.9	2.3	----	----	3.9	2.3	30.0	----	39	---
4415	0	.730	.625	.705	.105	.025	1.8	.6	.1	.3	1.7	.3	19.0	----	38	---
		.810	.625	.705	.185	.105	3.7	2.2	.6	1.8	3.1	.4	16.0	29.0	49	34
	2	.680	.590	.745	.090	----	1.5	.4	----	----	1.5	.4	23.0	----	35	---
		.790	.590	.745	.200	.045	4.1	2.6	.1	.6	4.0	2.0	20.5	----	47	---
	4	.650	.555	.780	.095	----	1.6	.5	----	----	1.6	.5	27.0	----	34	---
		.735	.555	.780	.180	----	3.6	2.0	----	----	3.6	2.0	25.0	----	41	---

FIGURE 1 — Effective change in upper surface angle of attack occasioned by the upper surface shock, $\Delta\alpha_{(U.S.S.)_U}$, degrees

Legend:
- $\left(\dfrac{dM_{cr}}{d\alpha}\right) \leq 0.025$
- $\left(\dfrac{dM_{cr}}{d\alpha}\right) > 0.025$

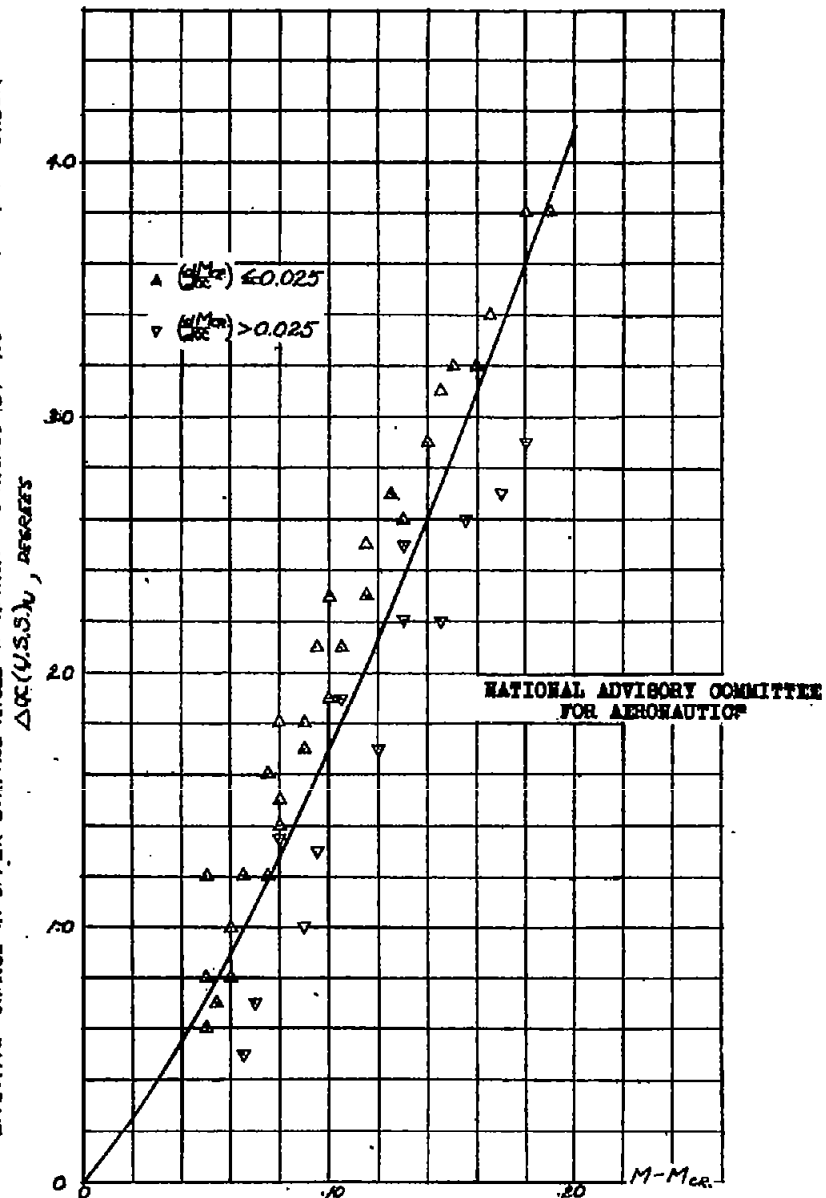NATIONAL ADVISORY COMMITTEE
FOR AERONAUTICS

$M - M_{cr}$

FIGURE 1.— EFFECTIVE CHANGE IN UPPER SURFACE ANGLE OF ATTACK WITH INCREMENT OF MACH NUMBER ABOVE THE CRITICAL.

FIGURE 2 — Effective change in lower surface angle of attack occasioned by the upper surface shock, $\Delta\alpha_{(U.S.S.)_L}$, degrees

Legend:
- $\left(\dfrac{dM_{cr}}{d\alpha}\right) \leq 0.025$
- $\left(\dfrac{dM_{cr}}{d\alpha}\right) > 0.025$

$M - M_{cr}$

FIGURE 2.— EFFECTIVE CHANGE IN LOWER SURFACE ANGLE OF ATTACK WITH INCREMENT OF MACH NUMBER ABOVE THE CRITICAL.

NATIONAL ADVISORY COMMITTEE
FOR AERONAUTICS
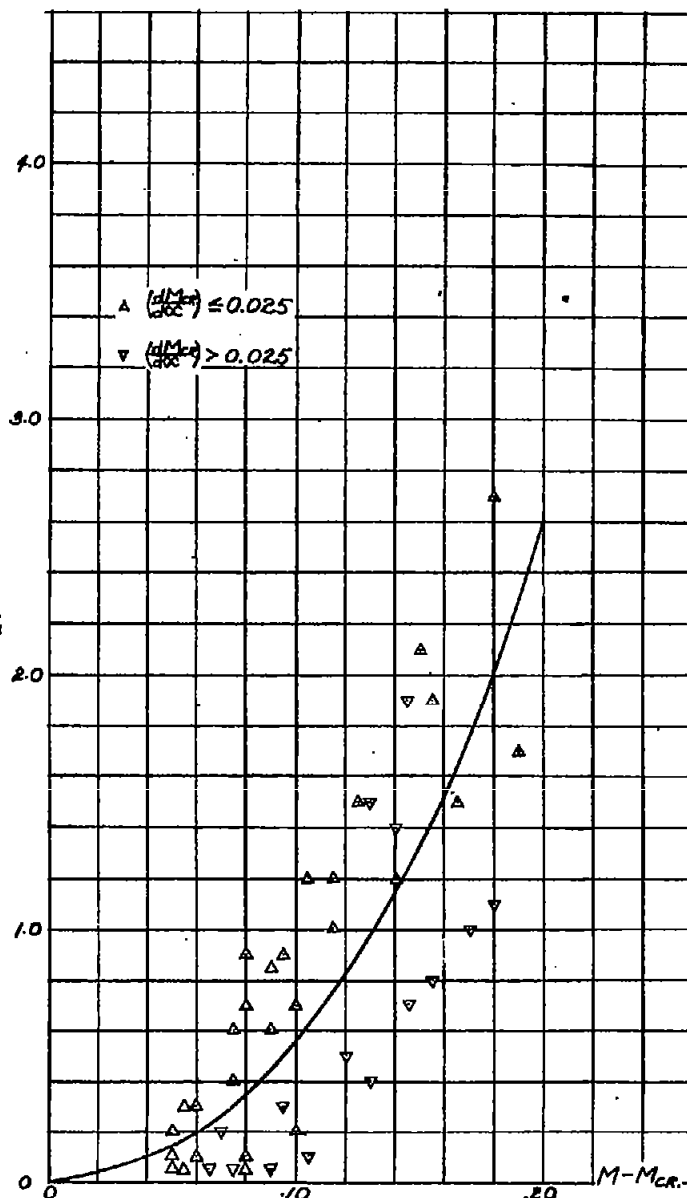
DRAG COEFFICIENT, AT M, MINUS LOW-SPEED DRAG COEFFICIENT, $C_D - C_{D_{L.S.}}$

$\triangle \; \left(\frac{dM_{cr}}{d\alpha}\right) \leq 0.025$

$\triangledown \; \left(\frac{dM_{cr}}{d\alpha}\right) > 0.025$

.08

.07

.06

.05

.04

.03

.02

.01

0

0   .10   .20 $M-M_{cr}$
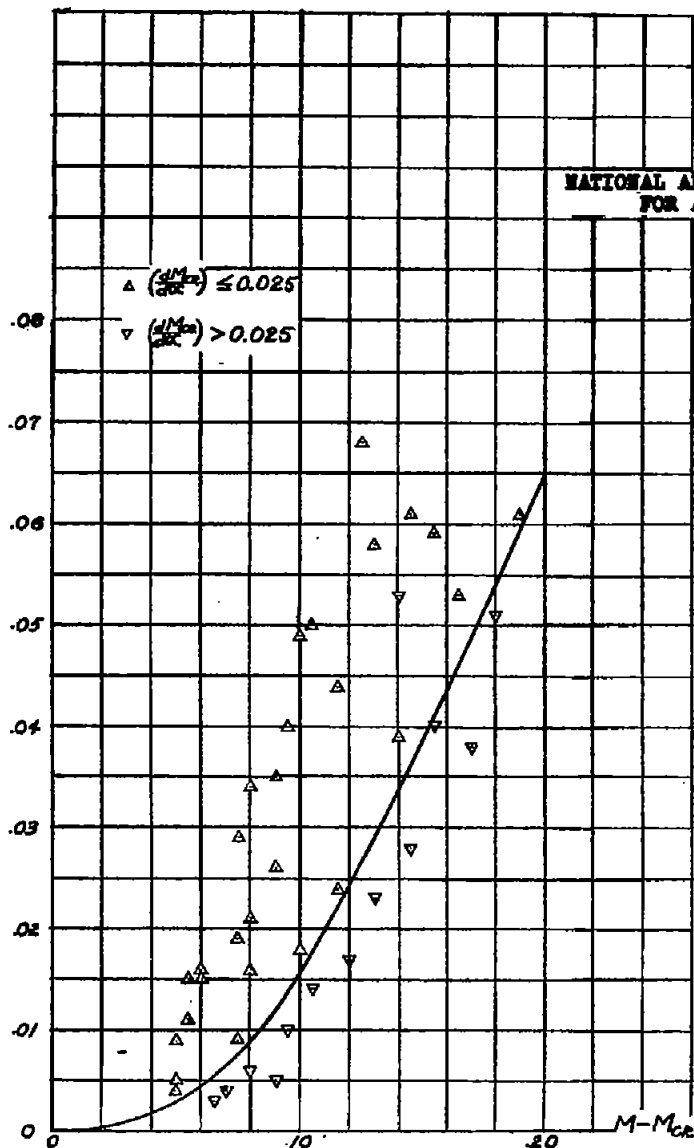
FIGURE 3.- DRAG COEFFICIENT INCREASE FOR MACH NUMBER
INCREMENTS ABOVE THE CRITICAL AT MODERATE
ANGLES OF ATTACK.

THEORY
EXP.   ○ □ △

1.000

.900

M_{cr}

.800

.700   NACA 66₂-215

NACA 65₂-215

.600   NACA 4412

-2   0   2   4 α
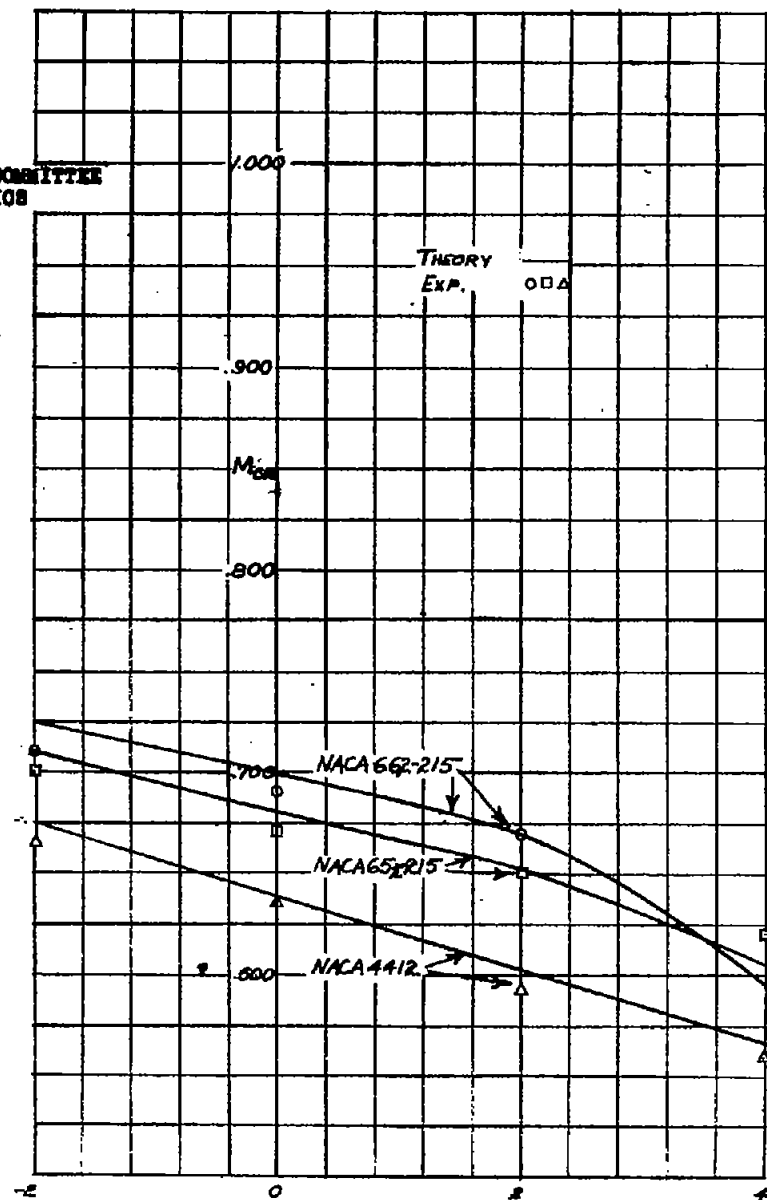
FIGURE 4.- VARIATION OF CRITICAL MACH NUMBER WITH ANGLE OF ATTACK,
(a) UPPER SURFACE : NACA 65₂-215, 66₂-215, AND 4412 AIRFOILS.

NATIONAL ADVISORY COMMITTEE
FOR AERONAUTICS
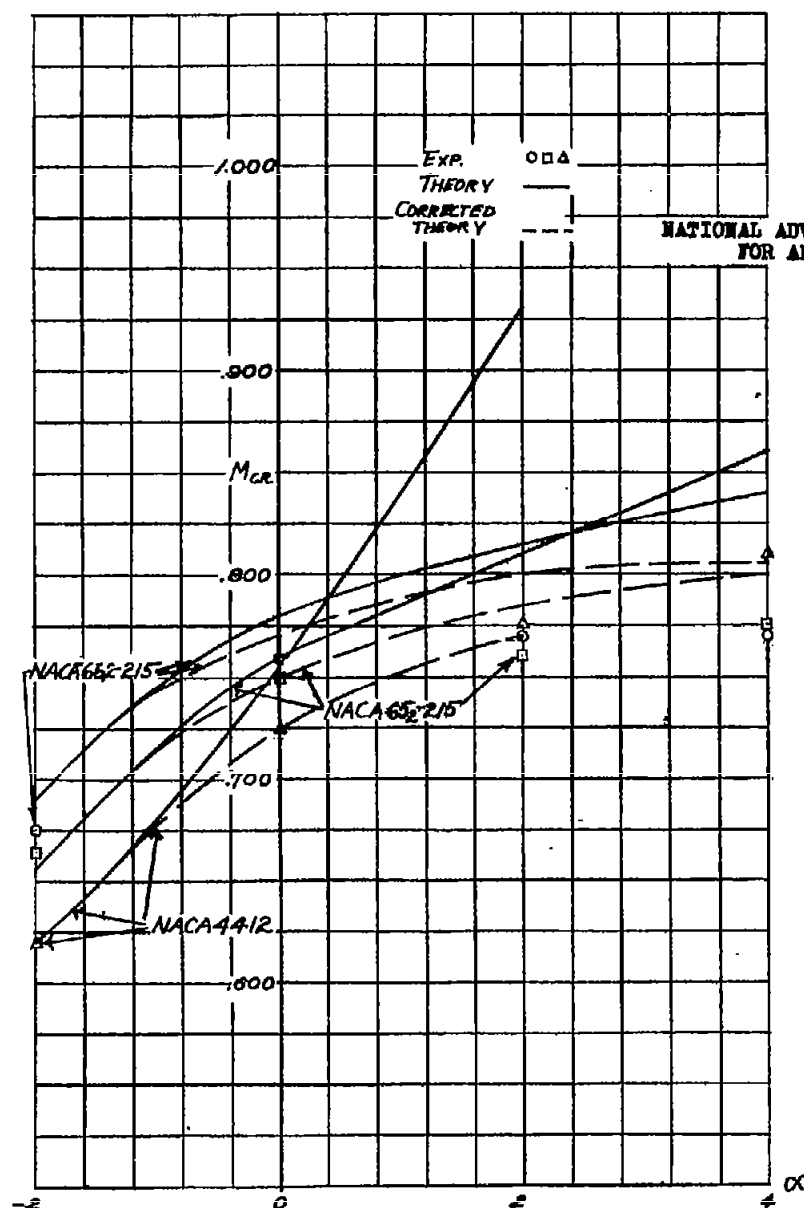
FIGURE 4.- (CONTINUED), CRITICAL MACH NUMBER
(b) LOWER SURFACE: NACA 65_2-215, 66,2-215 AND 4412 AIRFOILS
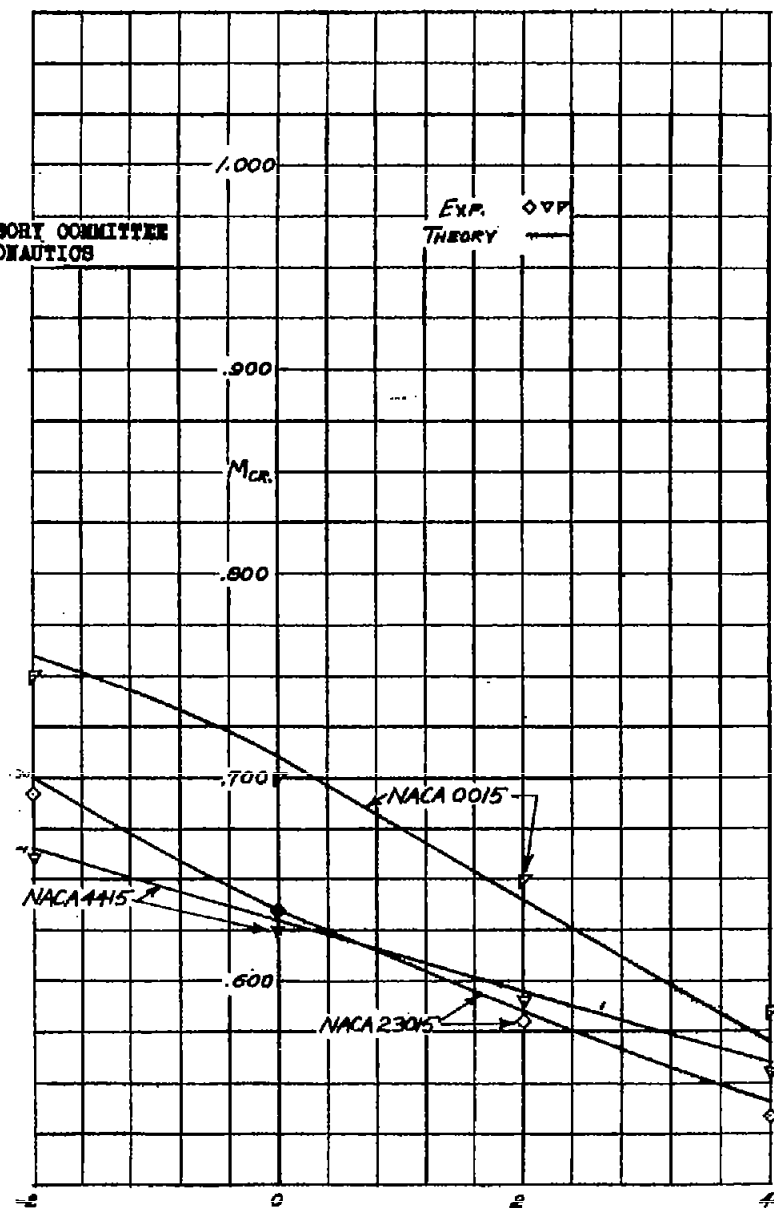
FIGURE 4.- (CONTINUED), CRITICAL MACH NUMBER
(c) UPPER SURFACE: NACA 0015, 23015, AND 4415 AIRFOILS
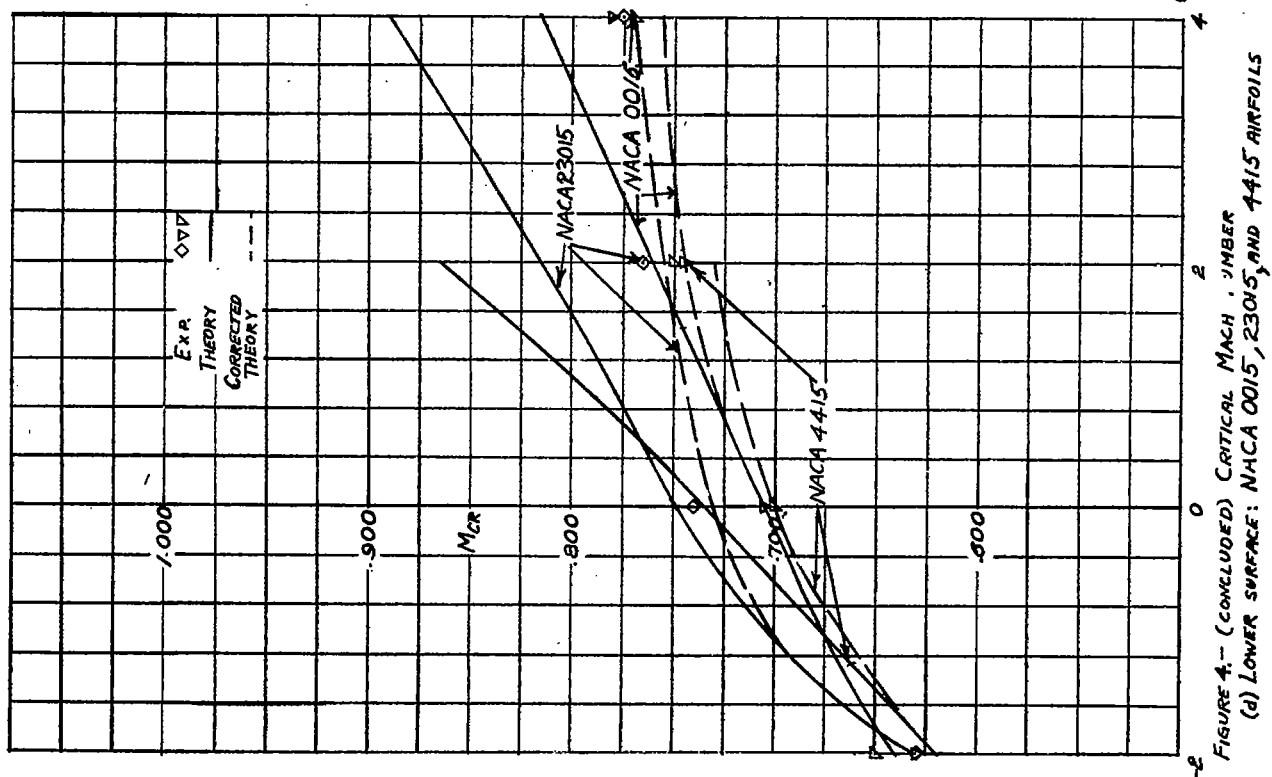
CONFIDENTIAL

FIGURE 4.— (CONCLUDED) CRITICAL MACH. NUMBER
(d) LOWER SURFACE: NACA 0015, 23015, AND 4415 AIRFOILS
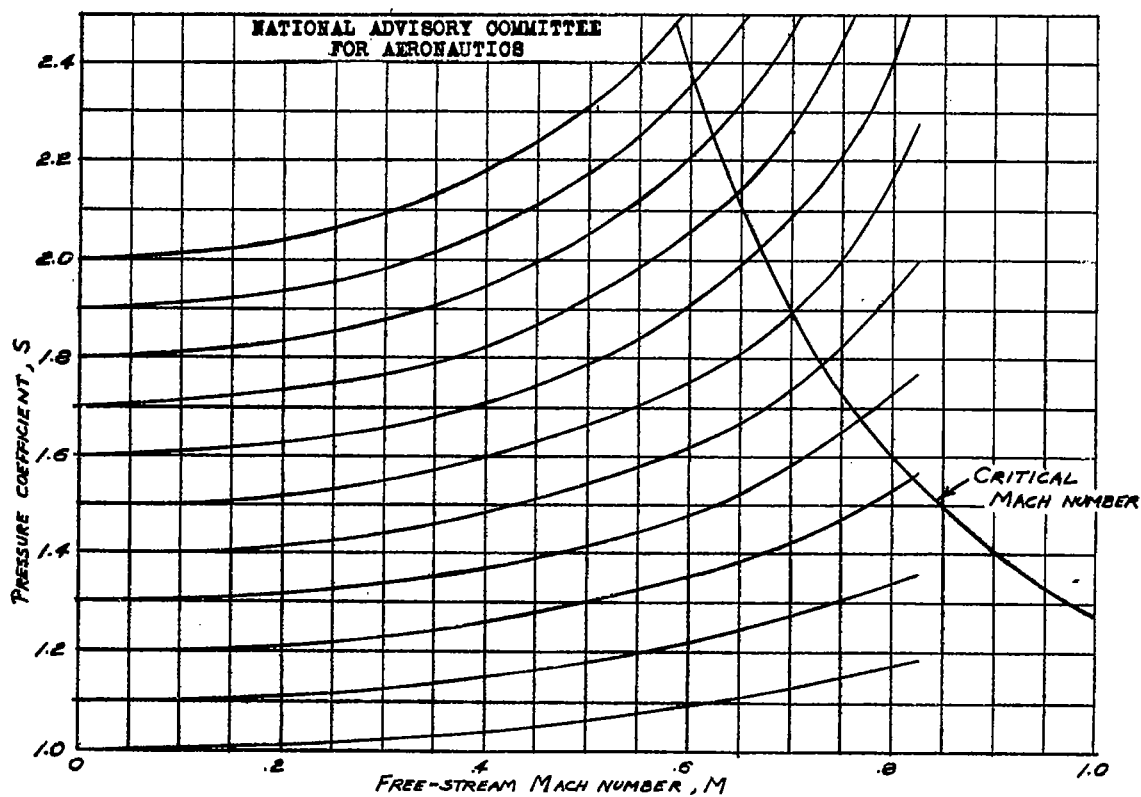
FIGURE 5.— KÁRMÁN-TSIEN THEORETICAL COMPRESSIBILITY CORRECTION FOR PRESSURE COEFFICIENTS.
CONFIDENTIAL
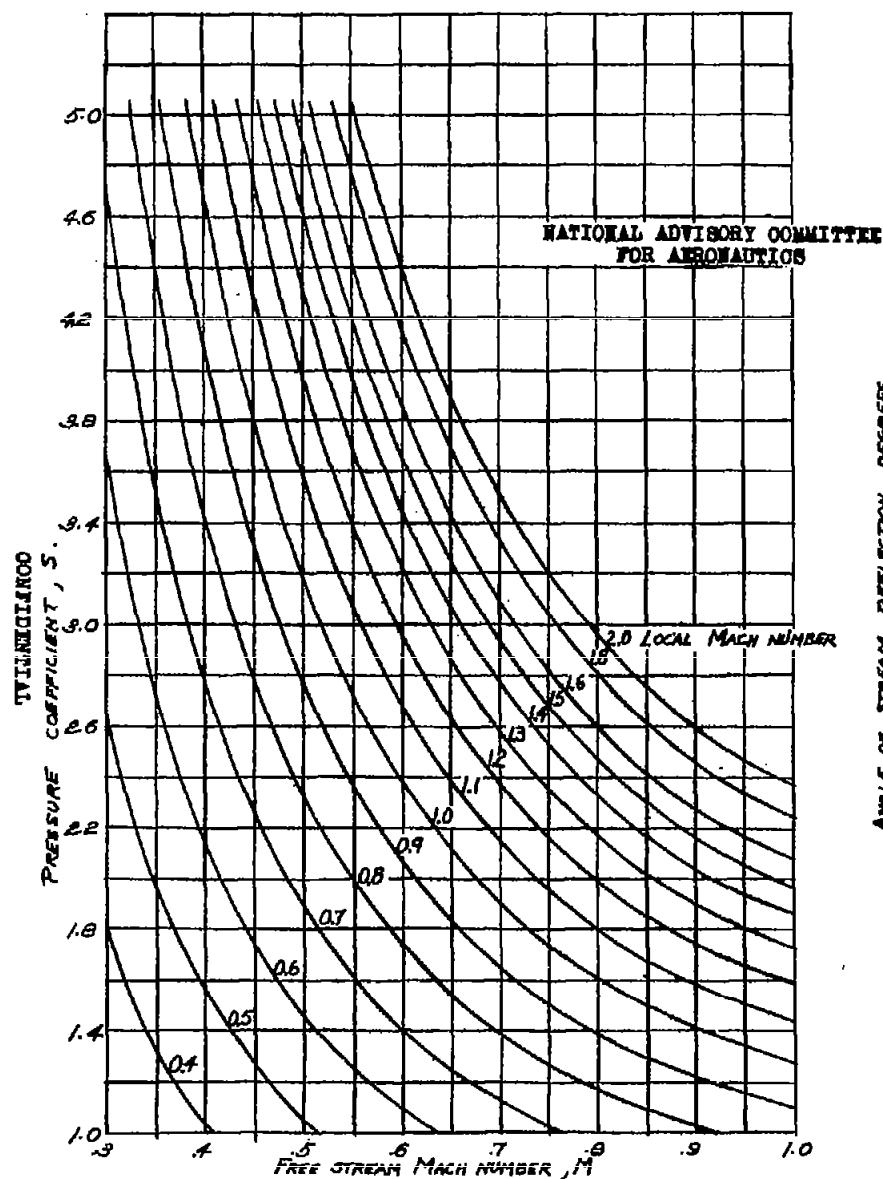
FIGURE 6.- VARIATION OF LOCAL MACH NUMBER WITH PRESSURE
COEFFICIENT AND FREE-STREAM MACH NUMBER.
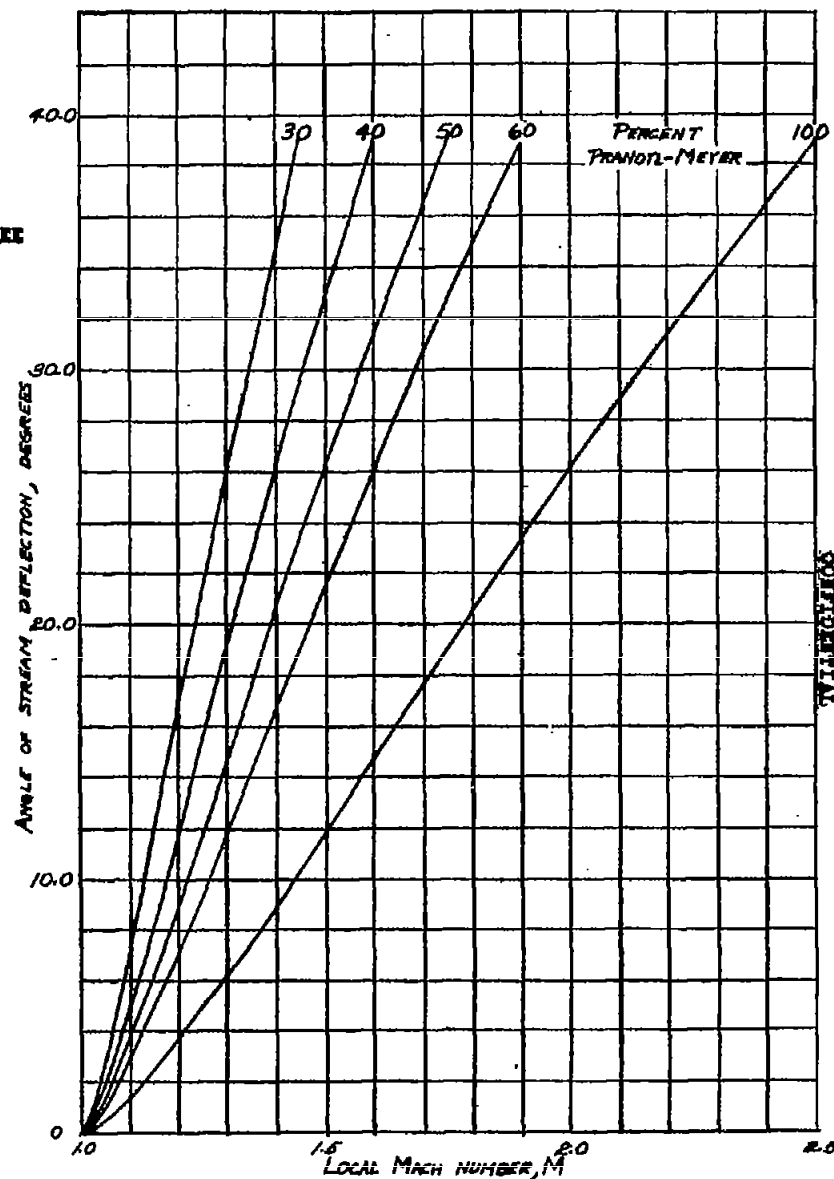
FIGURE 7.- PERCENTAGES OF PRANDTL - MEYER THEORETICAL
VARIATION OF LOCAL MACH NUMBER WITH ANGLE OF
STREAM DEFLECTION.
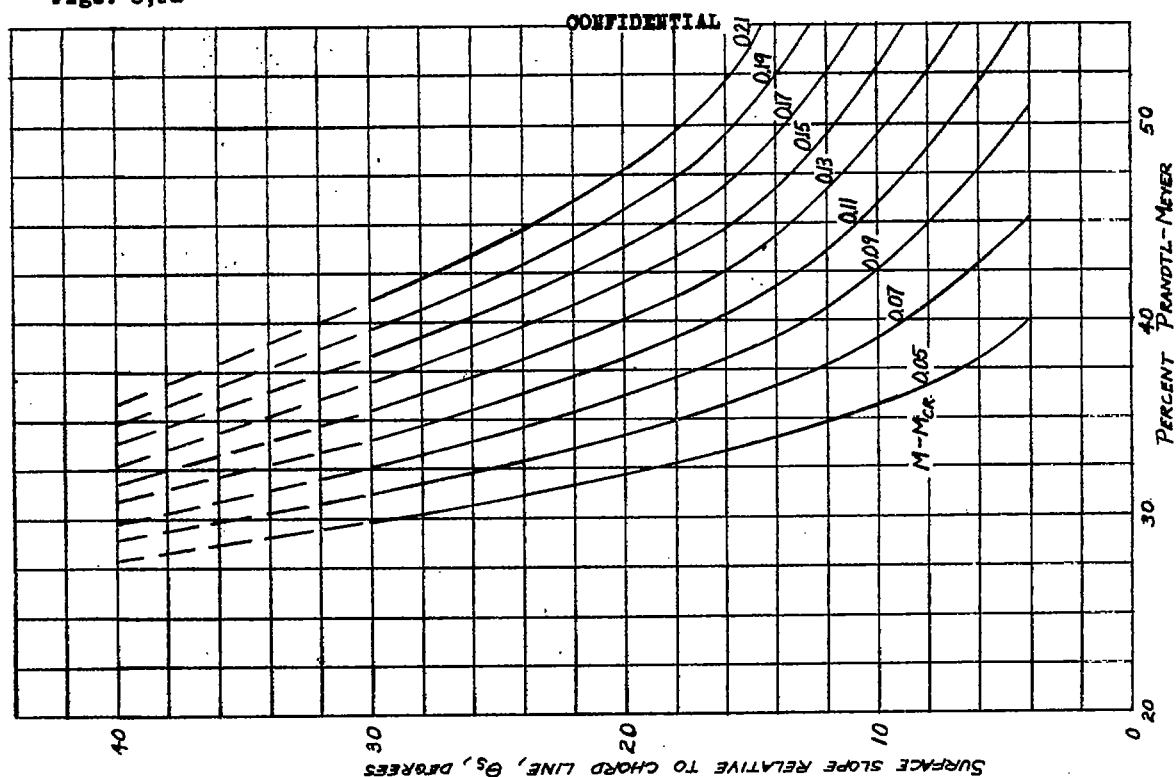
Figure 8.— Percent of Prandtl-Meyer theory attained for various values of $M-M_{cr}$ as a function of the airfoil surface slope at sonic point.

Figure 9.— Calculated and experimental pressure distributions for NACA 65,215 airfoil
(a) $\alpha = 2°$ M = 0.700 and 0.725

FIGURE 9.-(CONTINUED). NACA 65₂-215 AIRFOIL.
(b) α=2° ; M=0.750 AND 0.775

FIGURE 9.-(CONTINUED). NACA 65₂-215 AIRFOIL.
(c) α=2° ; M=0.800 AND 0.825.

CONFIDENTIAL
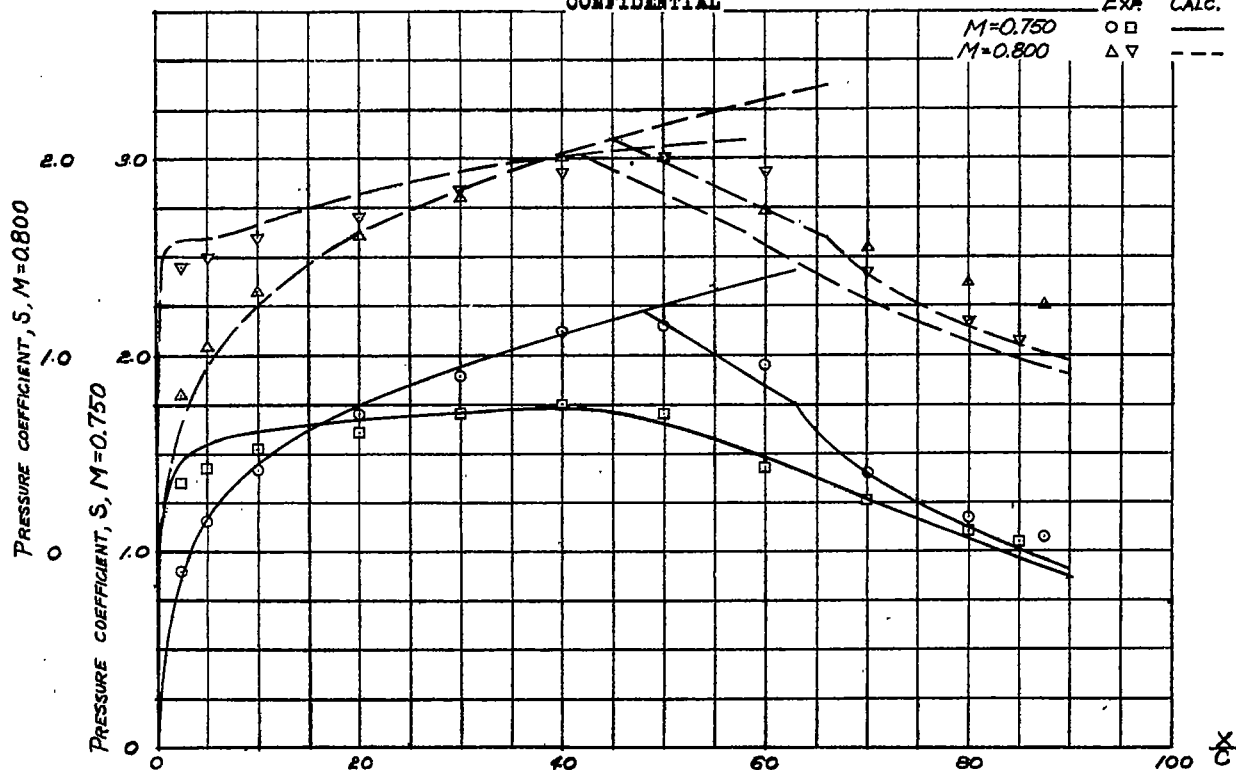
FIGURE 9.- (CONTINUED)   NACA 65₂-215 AIRFOIL
(d) α=0°   M=0.750 AND 0.800

NATIONAL ADVISORY COMMITTEE
FOR AERONAUTICS
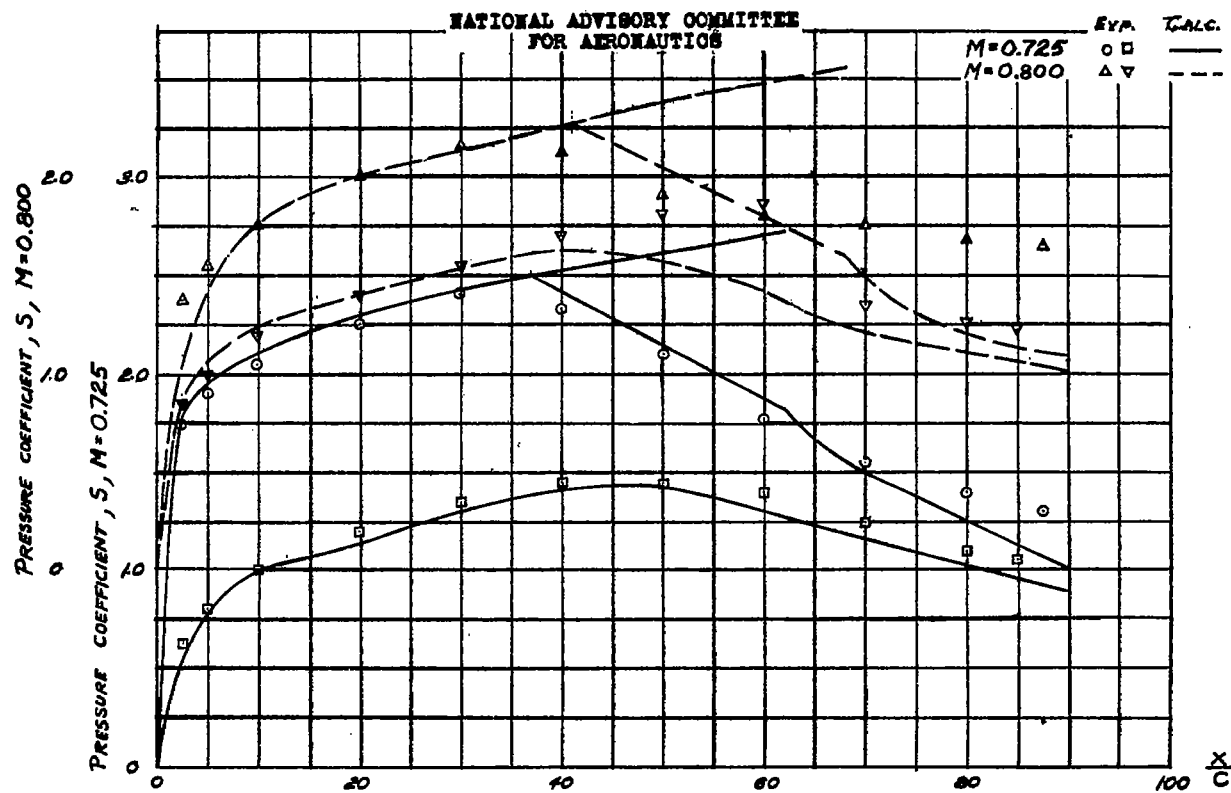
FIGURE 9.- (CONCLUDED)   NACA 65₂215 AIRFOIL
(e) α=4°   , M=0.725 AND 0.800.
CONFIDENTIAL
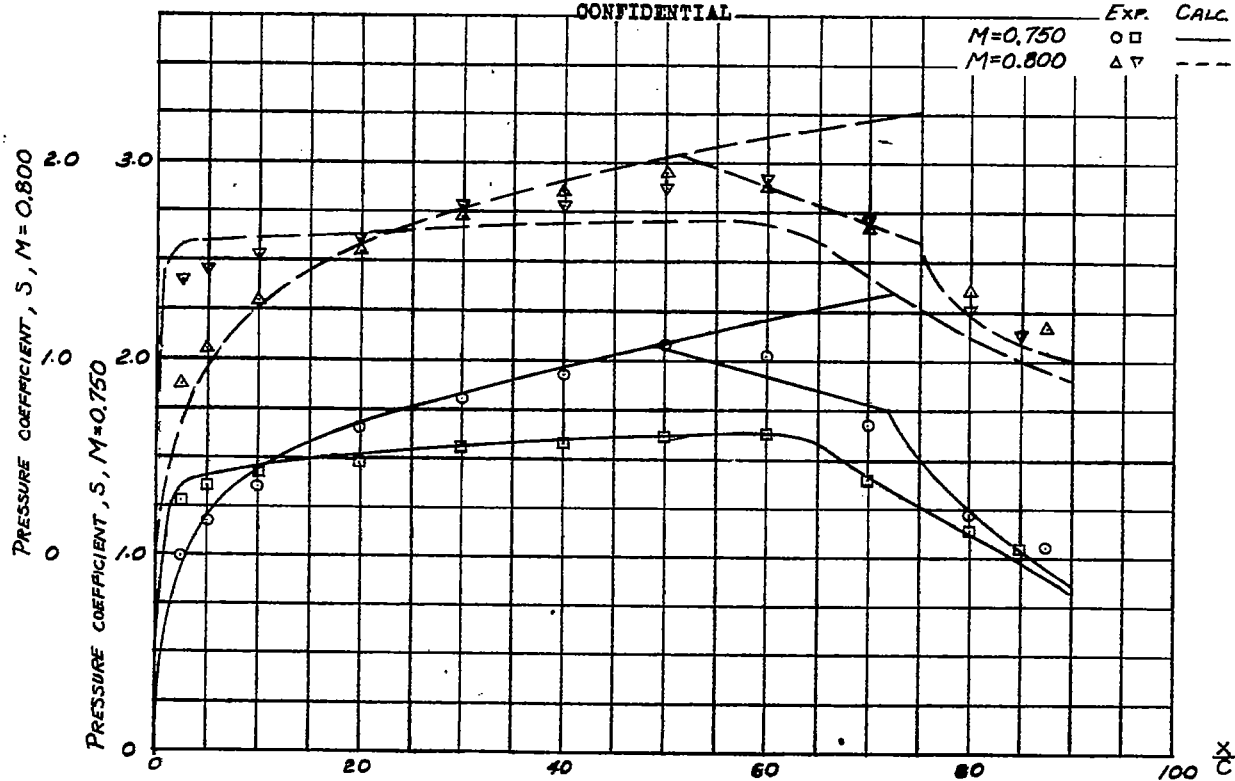
FIGURE 10.—CALCULATED AND EXPERIMENTAL PRESSURE DISTRIBUTIONS FOR NACA 66,2-215 AIRFOIL.
(a) ∝ = 0°   ; M=0.750 AND 0.800
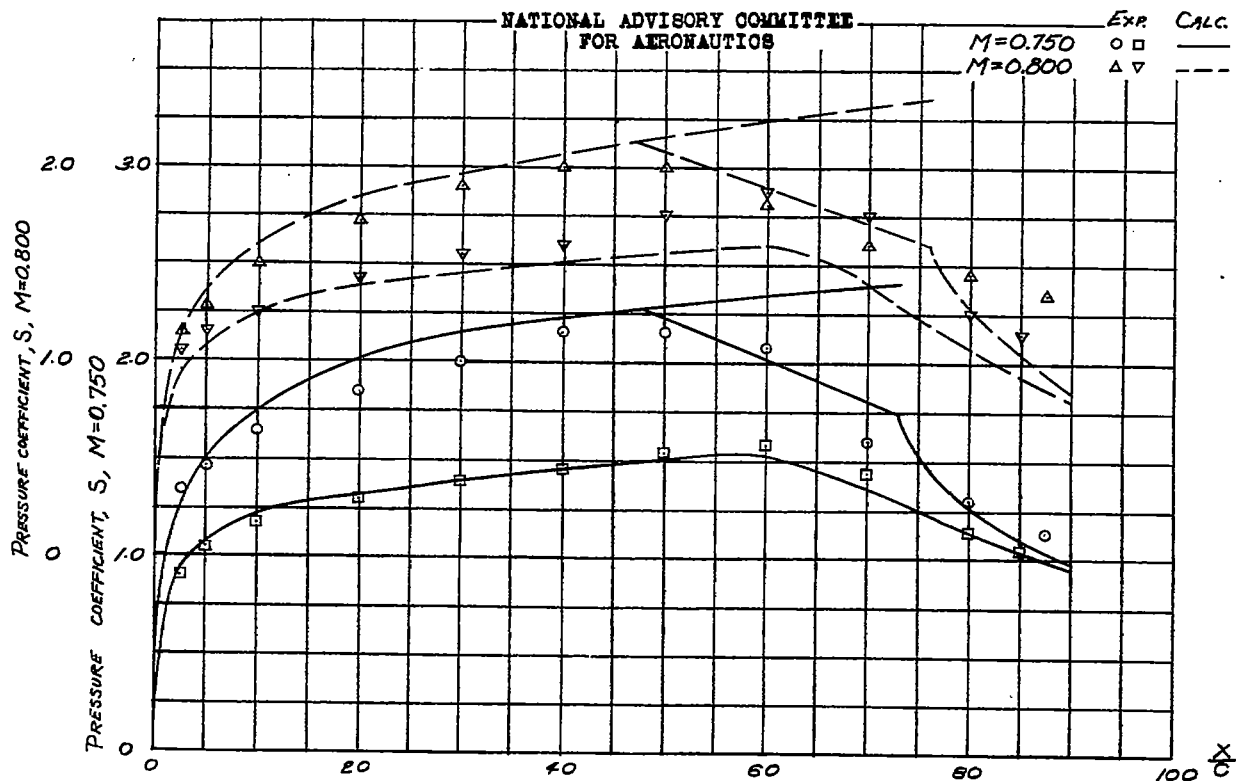
FIGURE 10.—(CONTINUED) , NACA 66,2-215 AIRFOIL.
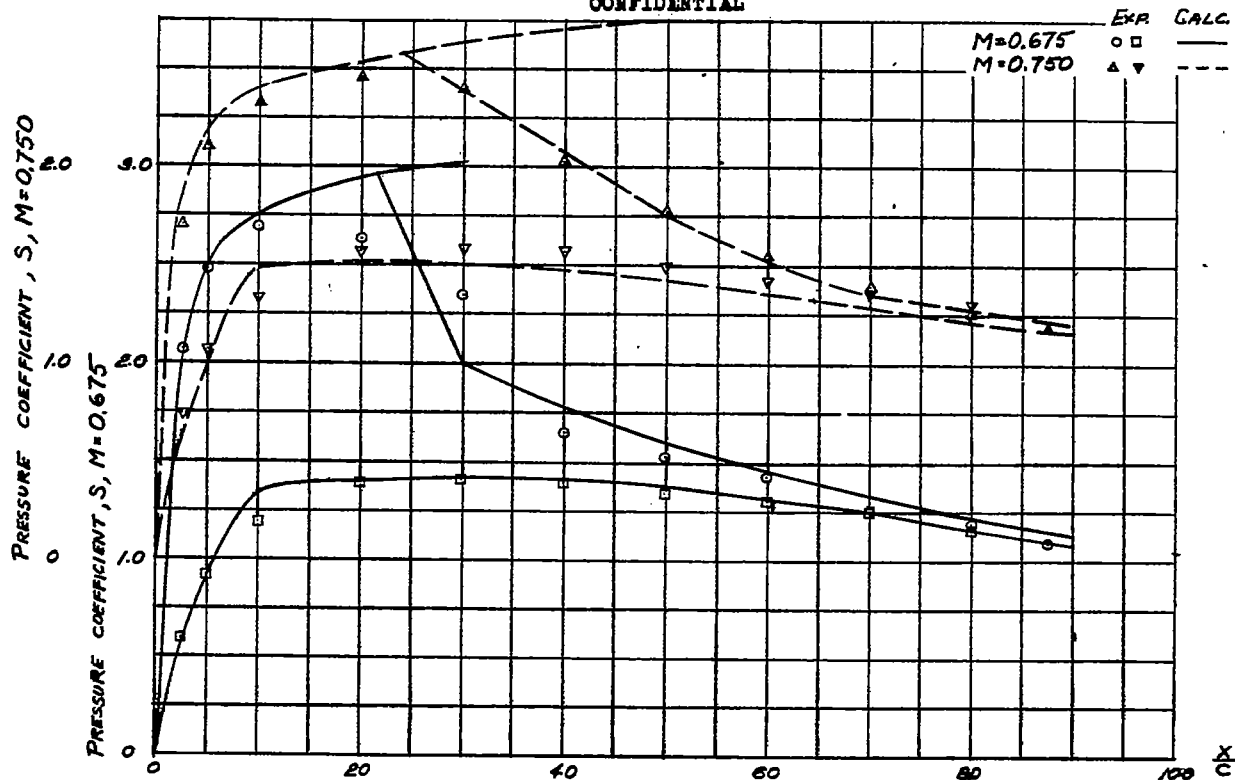(b) ∝ = 2° ; M=0.750 AND 0.800

CONFIDENTIAL
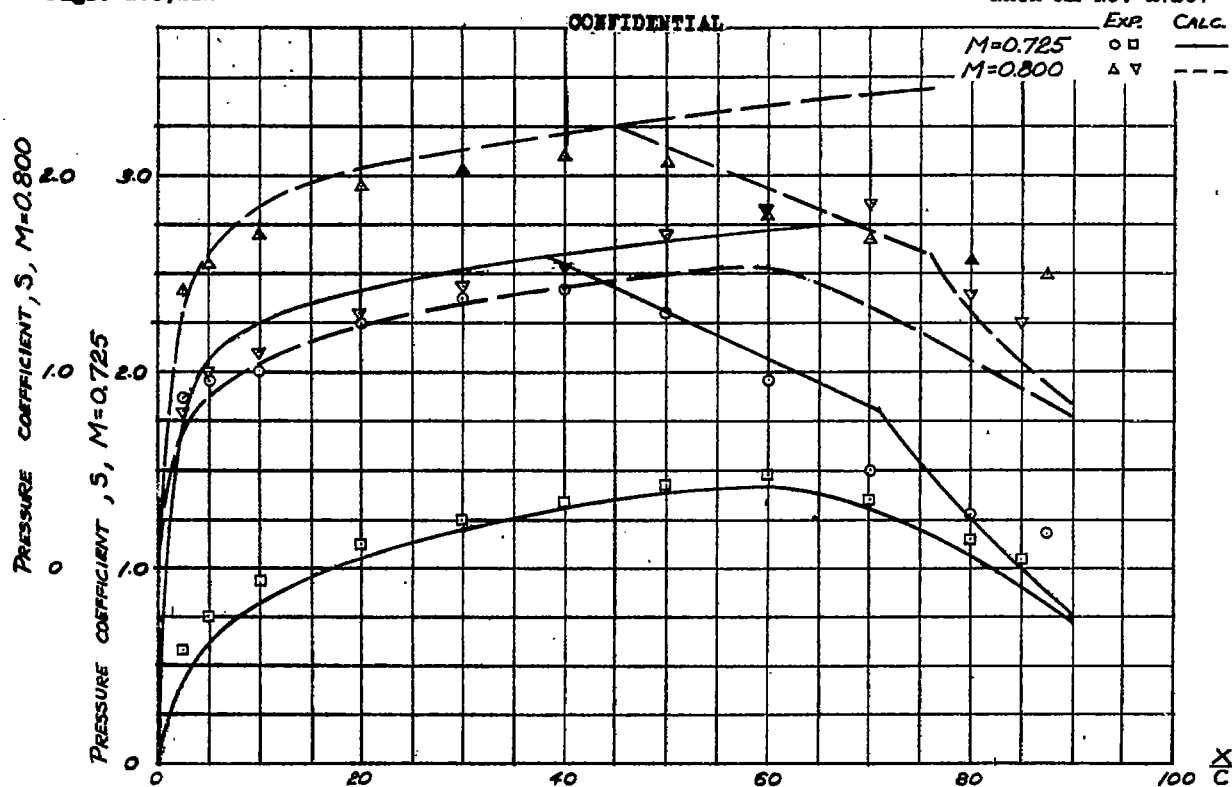
FIGURE 10.-(CONCLUDED) NACA 66,2-215 AIRFOIL
(c) $\alpha = 4°$; M=0.725 AND 0.800
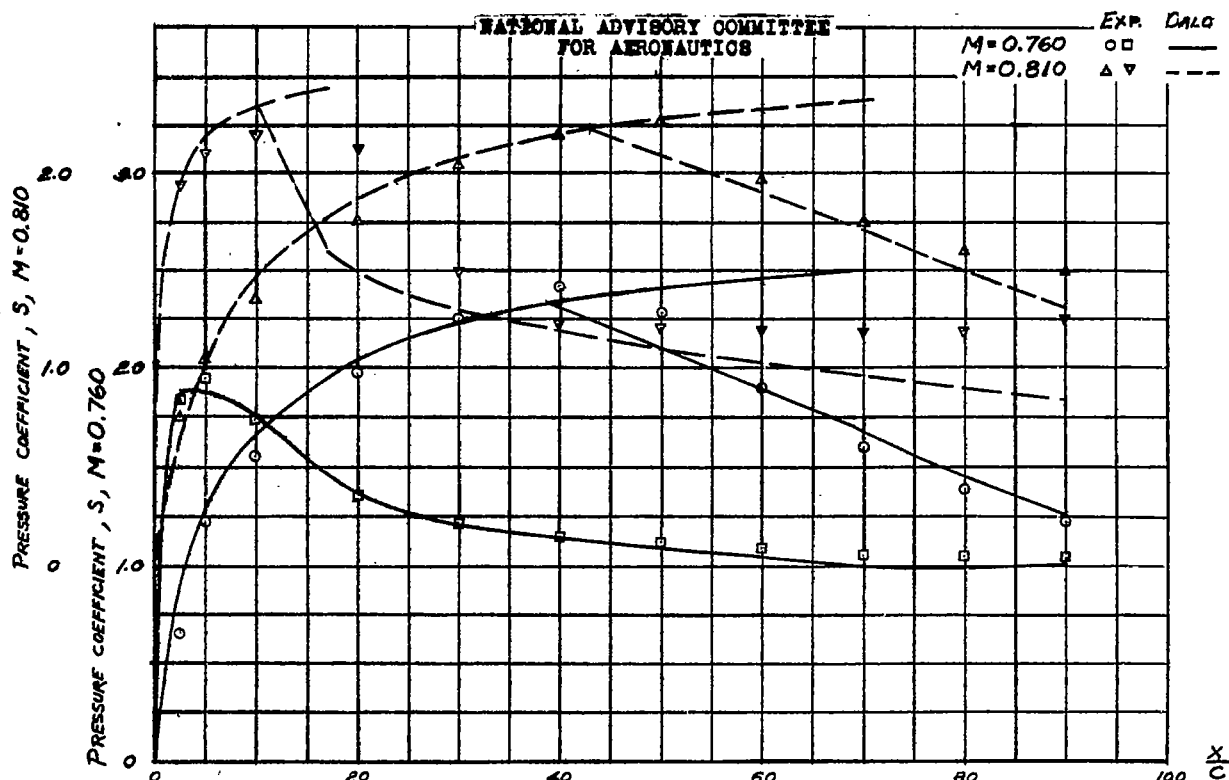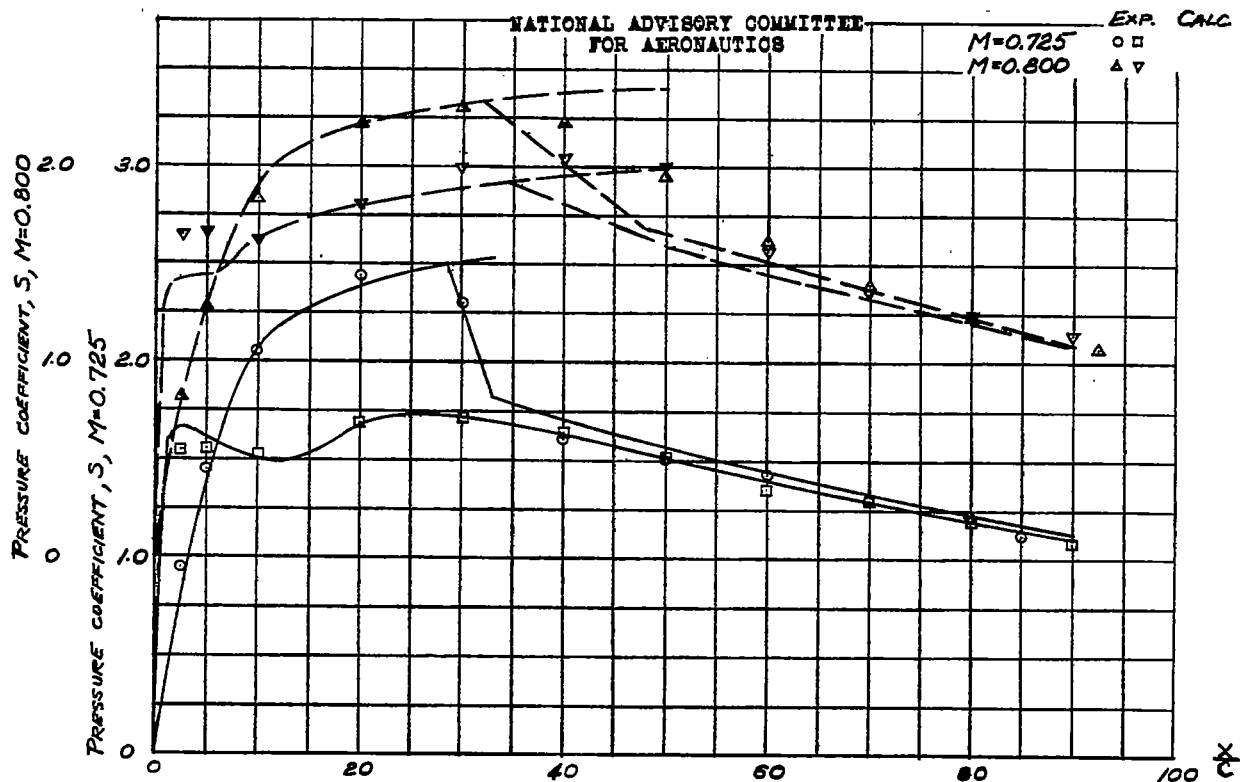

FIGURE 11.- CALCULATED AND EXPERIMENTAL PRESSURE DISTRIBUTIONS FOR NACA 4412 AIRFOIL
(a) $\alpha = 0°$; M=0.760 AND 0.810
CONFIDENTIAL

CONFIDENTIAL

FIGURE 11 - (CONTINUED). NACA 4412 AIRFOIL.
(b) α = 2°; M=0.700 AND 0.790.

FIGURE 11.- (CONCLUDED) NACA 4412 AIRFOIL
(c) α = 4°; M=0.650 AND 0.750
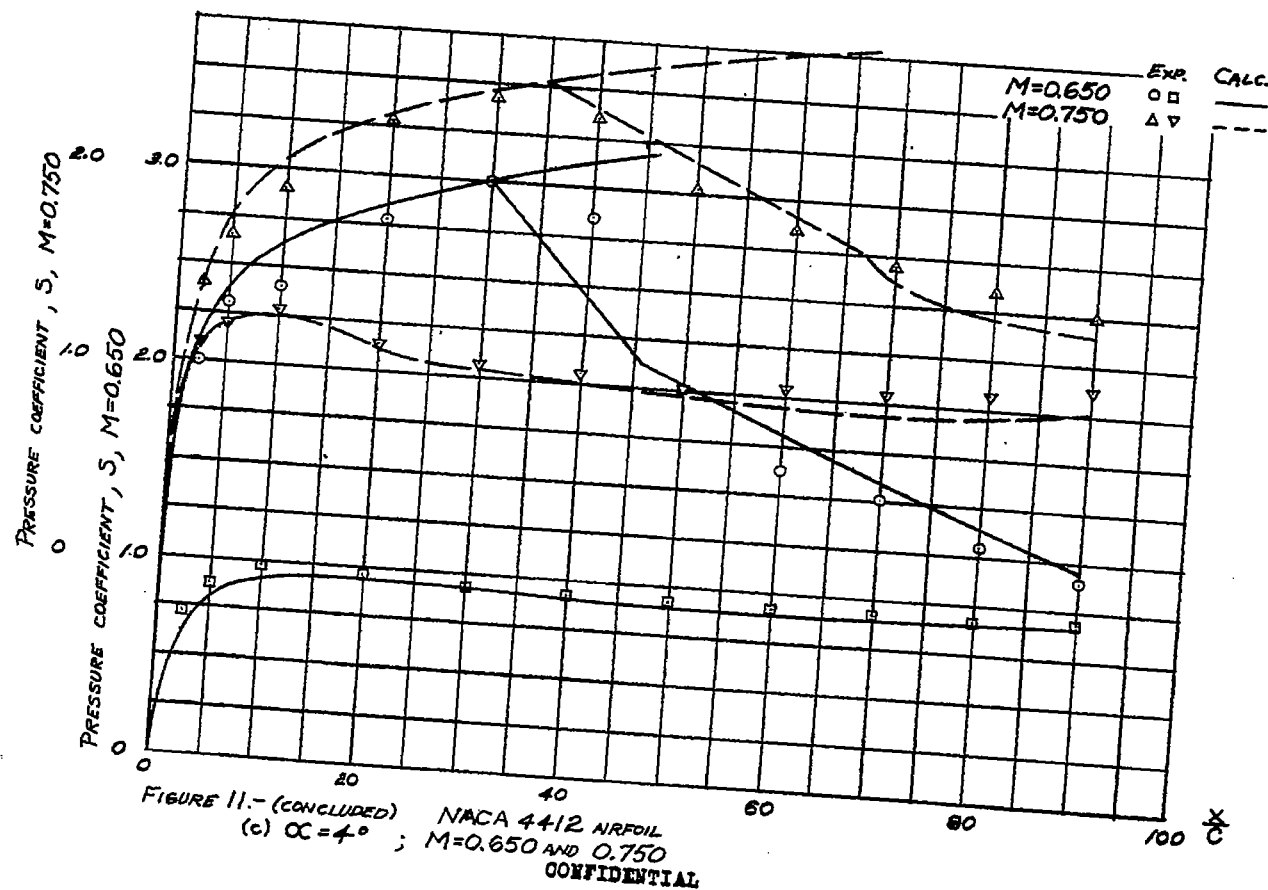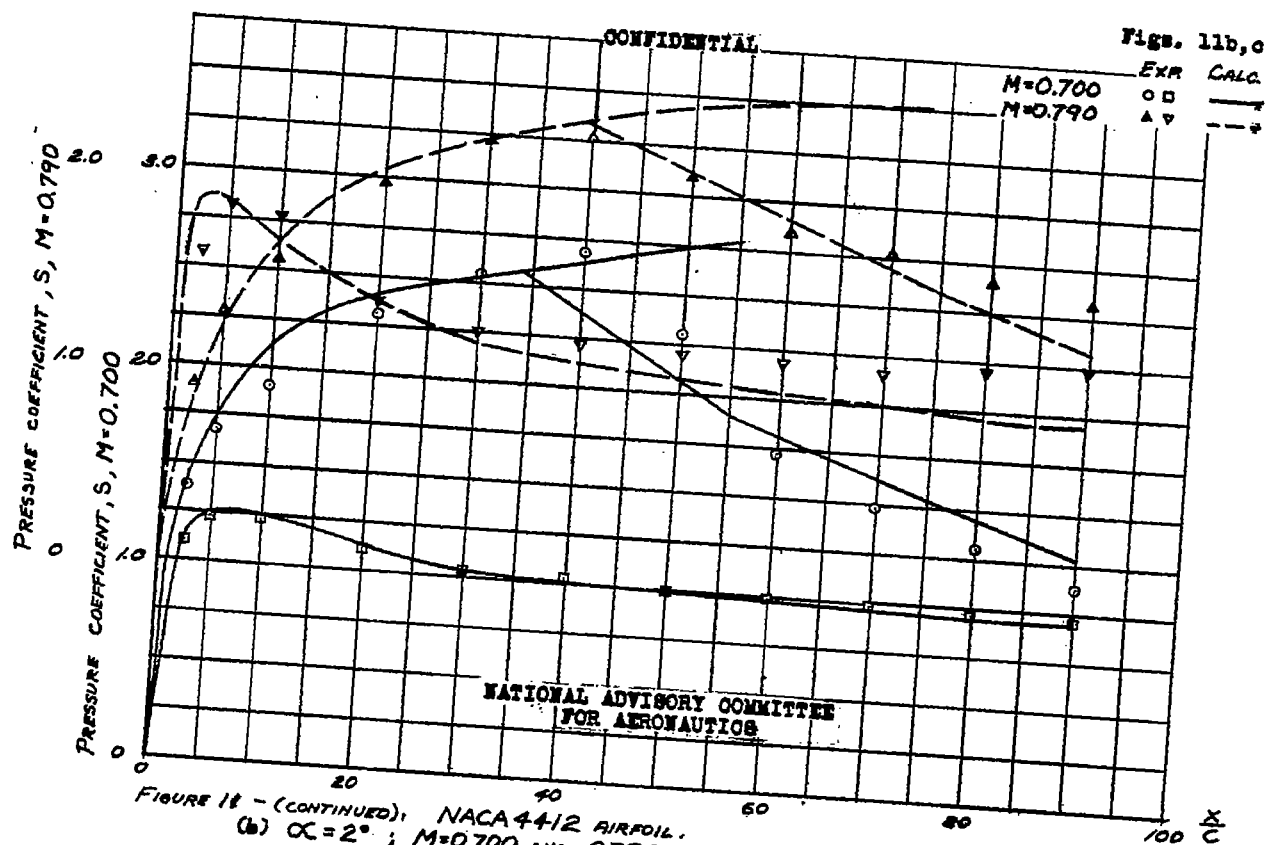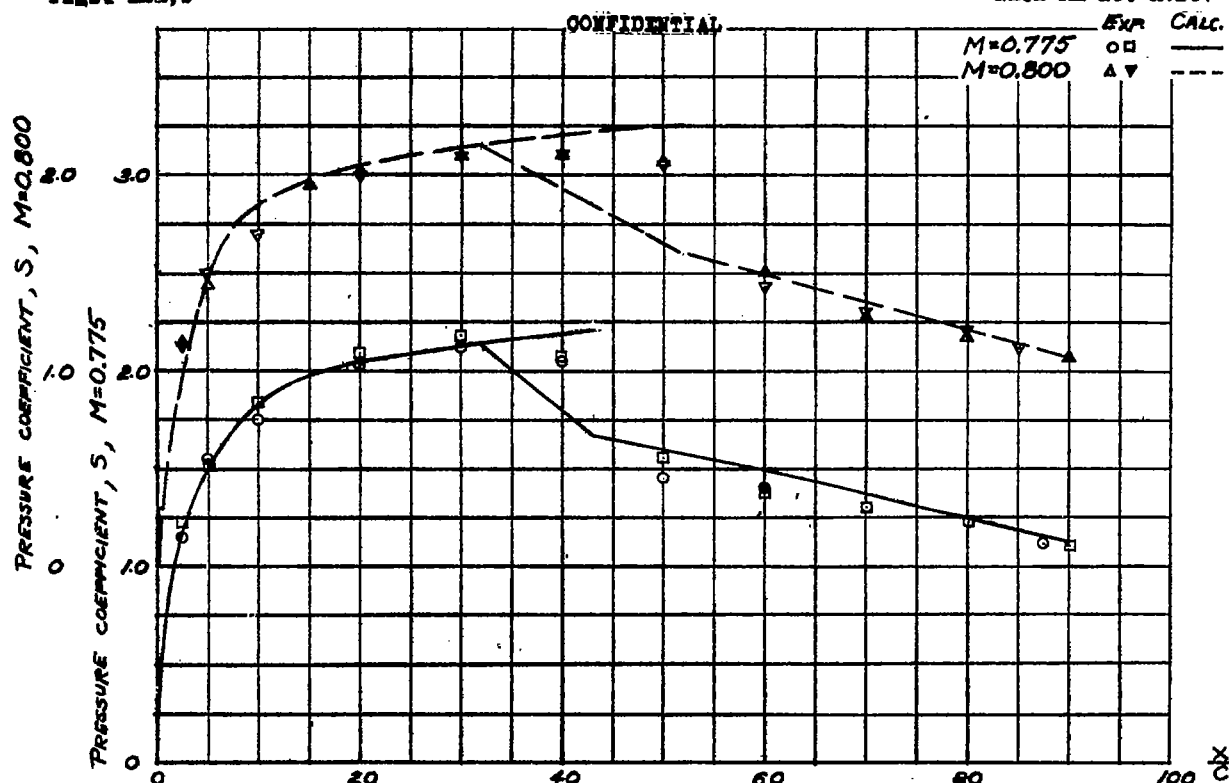
CONFIDENTIAL

FIGURE 12.— CALCULATED AND EXPERIMENTAL PRESSURE DISTRIBUTIONS FOR NACA 0015 AIRFOIL
(a) α = 0° ; M = 0.775 AND 0.800

FIGURE 12.— (CONTINUED)   NACA 0015 AIRFOIL
(b) α = 2° ; M = 0.725 AND 0.800

FIGURE 12.—(CONCLUDED) NACA 0015 AIRFOIL.
(c). α=4°; M=0.675 AND 0.750

FIGURE 13.—CALCULATED AND EXPERIMENTAL PRESSURE DISTRIBUTIONS FOR NACA 23015 AIRFOIL
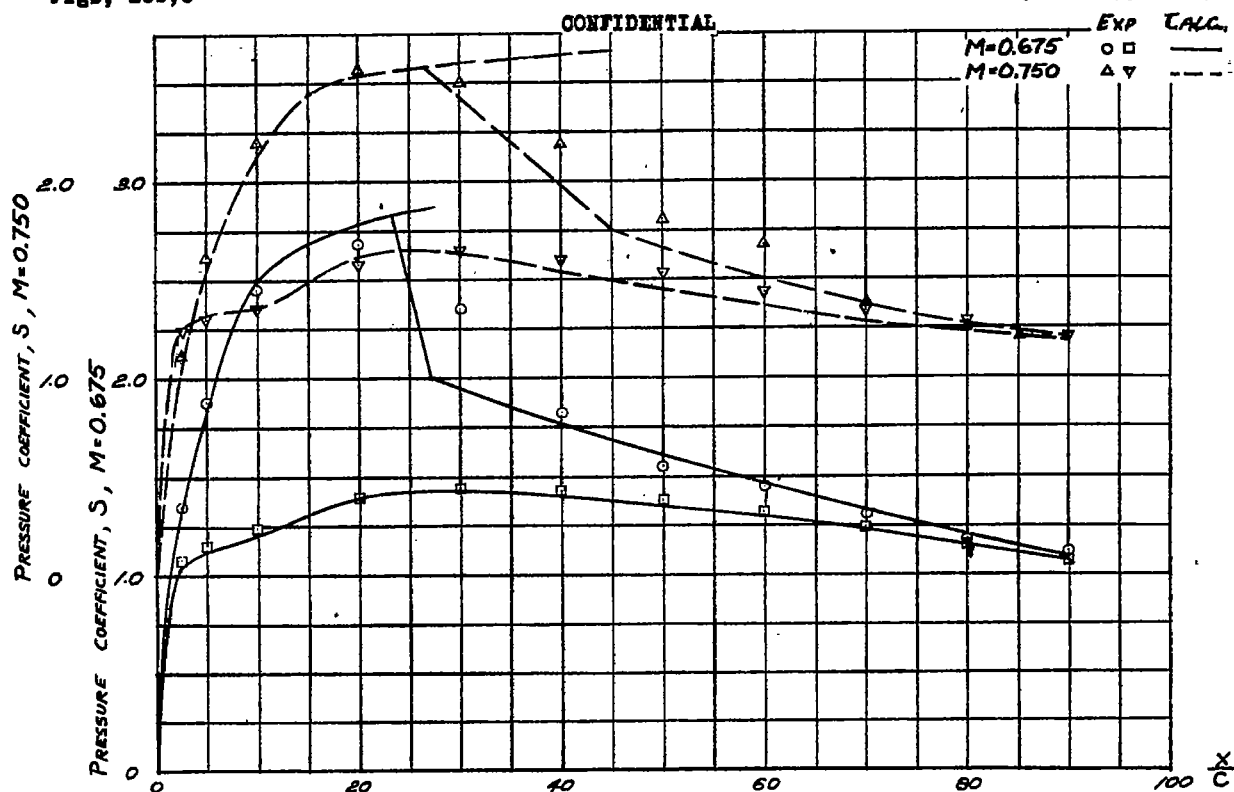(a) α=0°; M=0.725 AND 0.800

CONFIDENTIAL

CONFIDENTIAL

FIGURE 13.- (CONTINUED) NACA 23015 AIRFOIL
(b) ∝ = 2° ; M = 0.675 AND 0.750
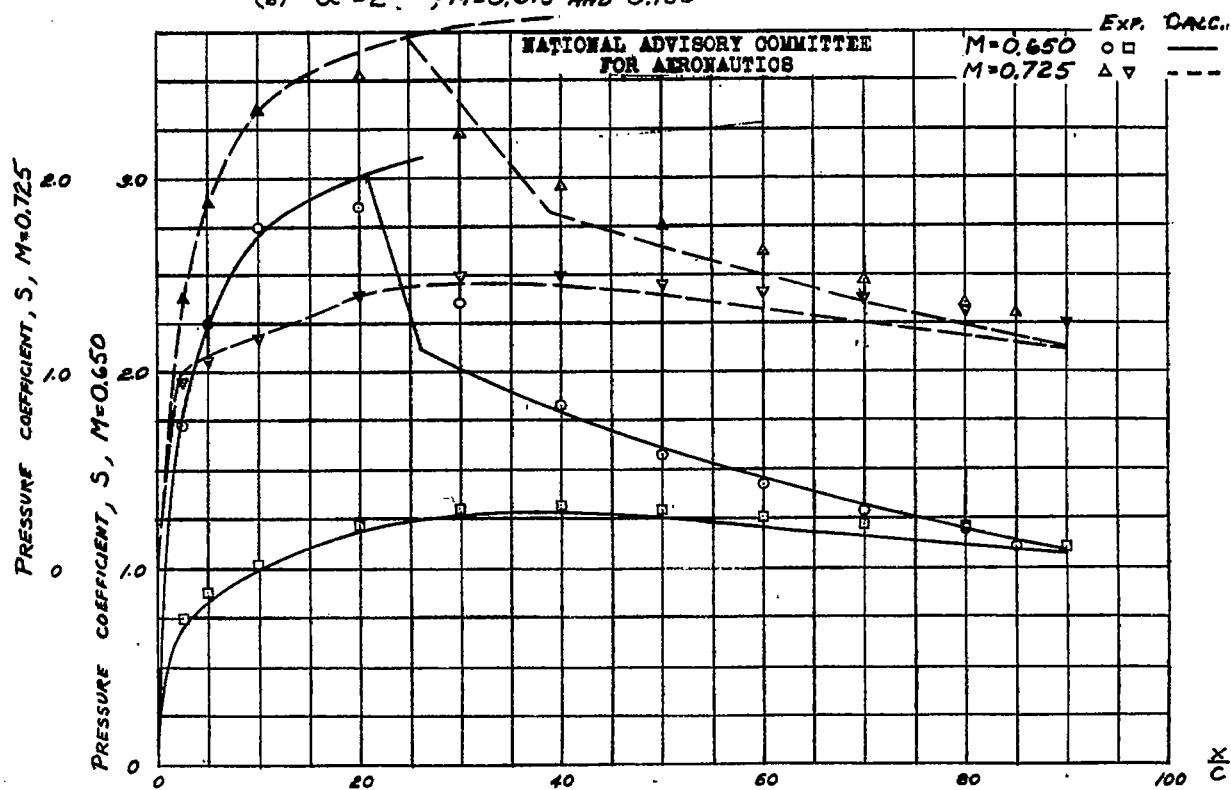
FIGURE 13.- (CONCLUDED) NACA 23015 AIRFOIL
(c) ∝ = 4° ; M = 0.650 AND 0.725

CONFIDENTIAL

CONFIDENTIAL

EXP. CALC.
M=0.730   o □   ———
M=0.810   △ ▼   - - -

PRESSURE COEFFICIENT, S, M=0.810

PRESSURE COEFFICIENT, S, M=0.730
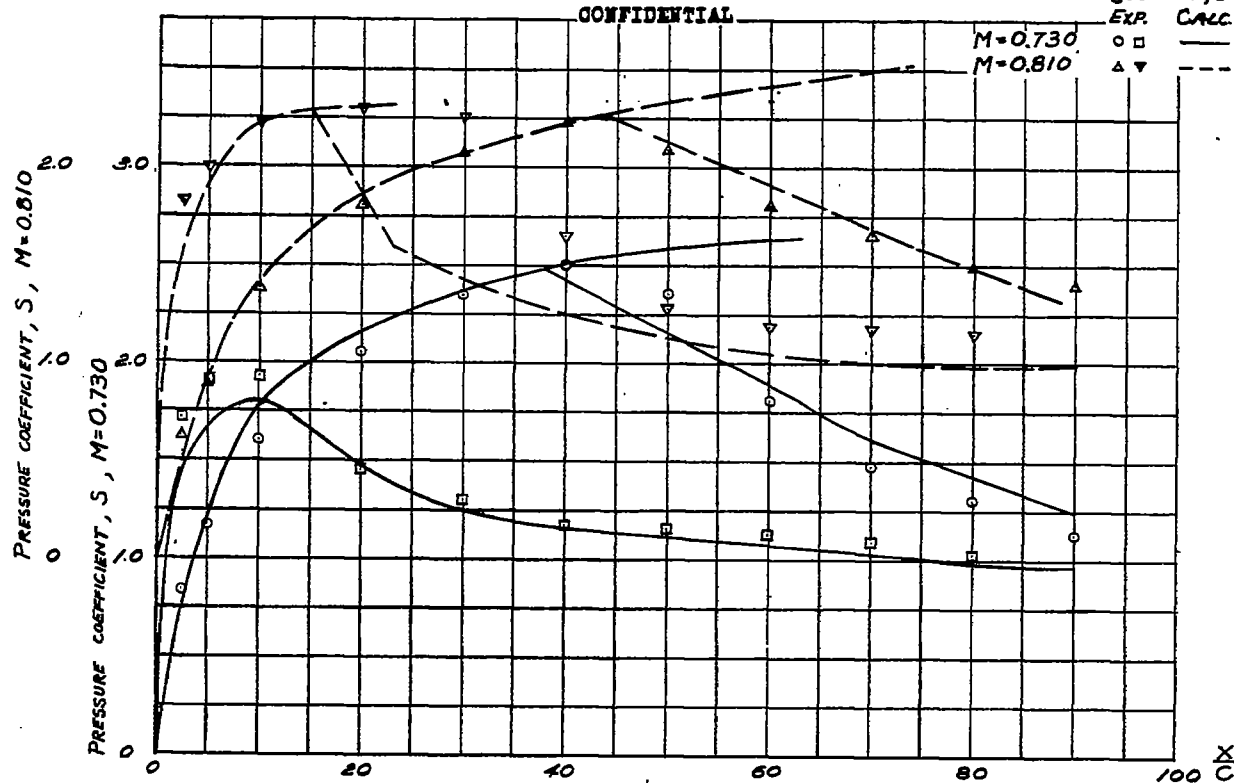
2.0   3.0

1.0   2.0

0   1.0

0

0   20   40   60   80   100   X/C

FIGURE 14.- CALCULATED AND EXPERIMENTAL PRESSURE DISTRIBUTIONS FOR NACA 4415 AIRFOIL
(a) α=0° ; M=0.730 AND 0.810

NATIONAL ADVISORY COMMITTEE
FOR AERONAUTICS

EXP. CALC.
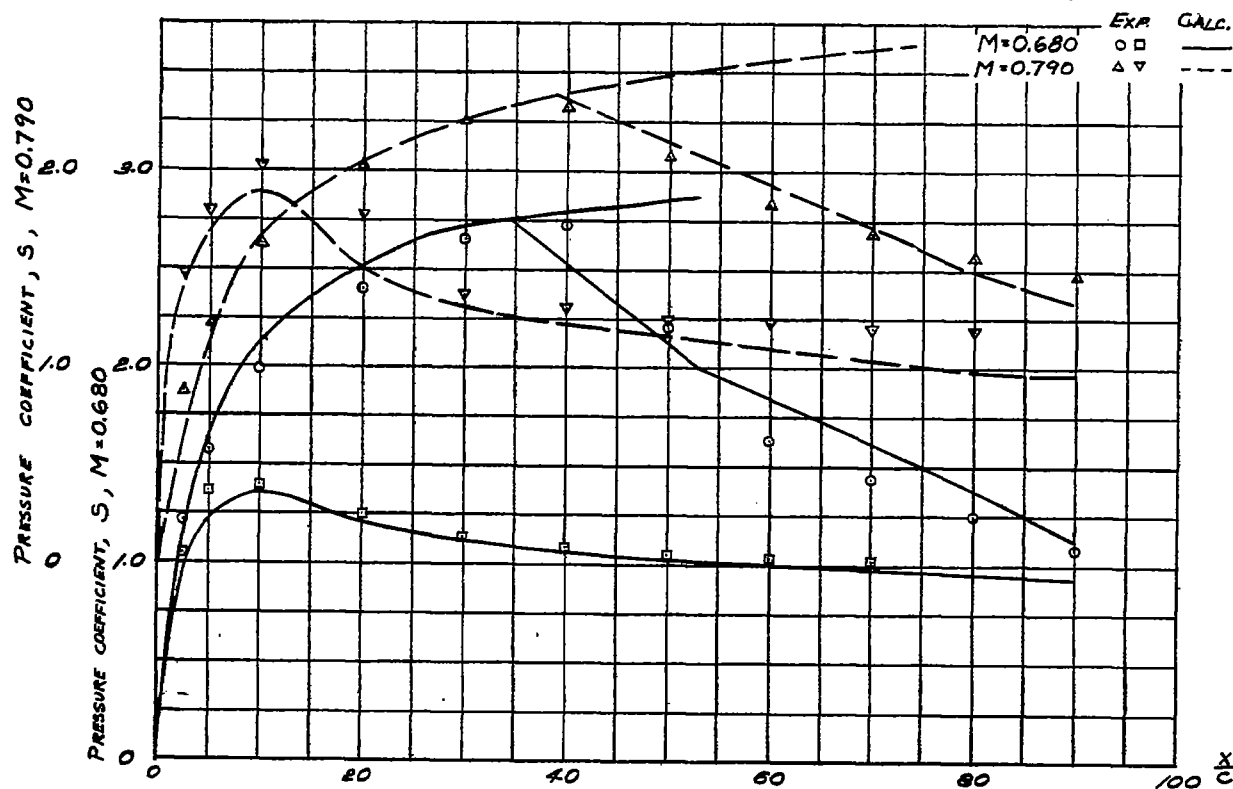M=0.680   o □   ———
M=0.790   △ ▼   - - -

PRESSURE COEFFICIENT, S, M=0.790

PRESSURE COEFFICIENT, S, M=0.680

2.0   3.0

1.0   2.0

0   1.0

0

0   20   40   60   80   100   X/C

FIGURE 14.- (CONTINUED) NACA 4415 AIRFOIL
(b) α=2° ; M=0.680 AND 0.790
CONFIDENTIAL

FIGURE 14.– (CONCLUDED) NACA 4415 AIRFOIL
(c) $\alpha = 4°$; M=0.650 AND 0.735

NACA RM No. A7B07